

**ELECTROPLATING OF Cu-Sn ALLOYS AND  
COMPOSITIONALLY MODULATED MULTILAYERS OF  
Cu-Sn-Zn-Ni ALLOYS ON MILD STEEL SUBSTRATE**

**by**

**HARIYANTI**

**Thesis submitted in fulfillment of the  
requirements for the degree of  
Master of Science**

**June 2007**

## **ACKNOWLEDGEMENTS**

I would like to take this opportunity to express my sincere gratitude and deep appreciation to my supervisor, Dr Sunara Purwadaria, for his invaluable insight, timely advice, and continual guidance. His scientific foresight and excellent knowledge have been crucial to the accomplishment of this work. I consider myself privileged for having had the opportunity to conduct research in the field of electroplating of Cu-Sn alloys under his supervision. Sincere appreciation and gratitude is addressed to Prof. Dr. Zainal Arifin Ahmad for allocating financial support from Malaysian Mining Chamber for this project, and making times for constructive discussion. I extend this acknowledgement to Assoc. Prof. Dr. Khairun Azizi Bt. Mohd. Azizli for her kind supports as a dean at the School of Materials and Mineral Resources Engineering.

Sincere thanks are given to all dedicated technical staffs, especially Mr. Sahrul, Ms. Fong and Mr. Rashid for their invaluable technical support, without these my research works cannot be completed properly as scheduled.

The inspiration and support given by the fellow postgraduate students of School of Materials and Mineral Resources Engineering have also been much appreciated.

Finally, I wish to express my deep gratitude to my parents, Moch Hari and Pudji Utami, my older brother Sutrisno, my younger brother Sugeng and Eko Pramono for their never-ending support, love, encouragement and always provided me the energy and enthusiasm for completing my work. I would like to dedicate the thesis to them.

## TABLE OF CONTENTS

	Page
<b>ACKNOWLEDGEMENTS</b>	ii
<b>TABLE OF CONTENTS</b>	iii
<b>LIST OF TABLES</b>	viii
<b>LIST OF FIGURES</b>	x
<b>LIST OF ABBREVIATION</b>	xvi
<b>LIST OF SYMBOLS</b>	xvii
<b>ABSTRAK</b>	xix
<b>ABSTRACT</b>	xxi
<b>CHAPTER 1 : INTRODUCTION</b>	1
1.1 Research Background	1
1.2 Research Objectives	4
1.3 Research Methodology	6
1.4 Expected Outcomes	14
<b>CHAPTER 2 : LITERATURE REVIEW</b>	15
2.1 Electroplating	15
2.2 Thermodynamic of Electrodeposition	19
2.2.1 Cathodic Processes	19
2.2.2 Anodic Processes	21
2.3 Kinetic and Mechanism of Electrodeposition Process	23
2.3.1 Relationship between Current and Potential	23
2.3.2 Influence of Mass Transport on Electrode Kinetics	25
2.3.3 Hydrogen Evolution	28
2.3.4 Atomic Aspects of Electrodeposition	29

2.3.5	Growth Mechanism	31
2.3.6	Development of Columnar Microstructure	35
2.4	Electrodeposition of Alloy	36
2.4.1	Structure of Electrodeposited Metal / Alloys	40
2.4.2	Properties of Electrodeposited Metal / Alloys	41
2.4.3	Corrosion of Electrodeposited Alloys	42
2.4.3.1	Corrosion of Coating-Substrate Systems	43
2.4.3.2	Electrochemical Corrosion Test	44
2.4.3.2	Dealloying	45
2.5	Electrodeposition of Copper-Tin Alloys	46
2.5.1	Cyanide System	46
2.5.2	Sulfate System	48
2.5.3	Plating Bath Selection	49
2.5.4	Properties of Copper-Tin Alloys	53
2.6	Electrodeposition of Multilayer	55
2.6.1	Compositionally Modulated Multilayer Alloy Applications	58
<b>CHAPTER 3 : PRELIMINARY EXPERIMENT</b>		62
3.1	Experimental Works	63
3.1.1	Preparation of Electroplating Baths	63
3.1.2	Preparation of Substrate	64
3.1.3	Polarization Measurement	65
3.1.4	Throwing Power Measurement	67
3.1.5	Study The Influence of Bath Composition and Current Density on The Composition, and The Uniformity of Cu-Sn Deposits	69
3.1.6	Characterization of Coating	71
3.1.6.1	Sample Preparation	71

3.1.6.2	Field Emission Scanning Electron Microscope (FE-SEM)	72
3.1.6.3	Energy Dispersive X-Ray Spectroscopy	73
3.1.6.4	X-Ray Diffraction	73
3.1.6.5	Microhardness Measurement	75
3.1.6.6	Corrosion Test	77
3.2	Result and Discussion of Preliminary Experiment	78
3.2.1	Introduction	78
3.2.2	Polarization Behavior	78
3.2.3	Throwing Power	84
3.2.4	Coating Composition and Electroplating Efficiency	86
3.2.5	Phase Analysis	89
3.2.6	Physical and Chemical Properties of Deposits	94
3.2.6.1	Surface Morphology	95
3.2.6.2	Coating Thickness Uniformity	99
3.2.6.3	Coating Microhardness	101
3.2.6.4	Corrosion Resistance of Binary Cu-Sn Coatings	102
	<b>CHAPTER 4 : PRODUCTION OF QUARTENARY YELLOW AND WHITE MIRALLOYS AND COMPOSITIONALLY MODULATED MULTILAYERS COATINGS</b>	107
4.1	Electroplating of Quarternary Cu-Sn-Zn-Ni Alloys	107
4.2	Electrodeposition of Compositionally Modulated Multilayers Coatings	109
4.3	Characterization of Coating	111
4.3.1	Sample preparation	111
4.3.2	Field Emission Scanning Electron Microscope Observation (FE-SEM)	111
4.3.3	Energy Dispersive X-Ray Spectroscopy	112
4.3.4	X-Ray Diffraction (XRD)	112

4.3.5	Mechanical Properties Measurements	113
4.3.5.1	Tensile Testing	113
4.3.5.2	Microhardness Measurement	116
4.3.6	Corrosion Test	116
4.4	Results and Discussion	117
4.4.1	Introduction	117
4.4.2	Coating Composition and Cathodic Current Efficiency	117
4.4.3	Phase Analysis	121
4.4.4	Physical and Chemical Properties of Deposits	123
4.4.4.1	Surface Morphology	124
4.4.4.2	Coating Thickness Uniformity	126
4.4.4.3	Influence of the present of Zn and Ni on the corrosion resistance of Yellow and White Miralloys Coatings	127
4.4.5	Production of Compositionally Modulated Multilayer Coating	129
4.4.5.1	Microhardness of Quarternary and CMM Coatings	133
4.4.5.2	Tensile Test	136
4.4.5.3	Fracture Surface	137
	<b>CHAPTER 5 : CONCLUSION AND RECOMMENDATION FOR FUTURE WORK</b>	140
5.1	Conclusion	140
5.2	Recommendation for Future Work	142
	<b>REFERENCES</b>	143
	<b>APPENDICES</b>	148
APPENDIX A	Potential–pH diagrams at 25°C	149
APPENDIX B	Calculation on Starting Materials Needed to Prepared Solution	150

APPENDIX C	Phase Diagram	153
APPENDIX D	Calculation on Cathodic Current Efficiency	154
APPENDIX E	The values of interplanar spacing (d) and the preference orientation	159
APPENDIX F	Results of Vickers Microhardness for Binary, Quarternary and Multilayer Alloy Coatings	160
APPENDIX G	Results of Corrosion Rate of Binary and Quarternary Alloy Coatings in 2 g/l H <sub>2</sub> SO <sub>4</sub> Solution	162
APPENDIX H	Results of Tensile Properties of Quarternary and Multilayer Alloy Coatings	163
<b>LIST OF PUBLICATIONS</b>		<b>164</b>

## LIST OF TABLES

	<b>Page</b>
2.1 Standard reduction electrode potentials at 25 °C [Gabe, 1978]	37
2.2 Vickers microhardness (HV) for selected metals [Kanani, 2004]	42
3.1 Concentration of dissolving species in the electroplating baths used for producing binary yellow and white alloys coating	62
3.2 Concentration of dissolving species in the electroplating baths used for polarization measurements	65
3.3 Composition of electrolyte for throwing power measurement	68
3.4 Throwing power from bath solution IV at temperature 65 °C	84
3.5 The values of interplanar spacing (d) and preference orientation for binary alloy coatings	92
3.6 Phase identification results in selected coatings	94
3.7 Average thickness of binary copper-tin alloy coating developed at different electroplating bath and current densities	100
3.8 Corrosion parameters of mild steel, copper and tin which are obtained from polarization measurement in 2 g/l H <sub>2</sub> SO <sub>4</sub>	103
3.9 Corrosion potentials and corrosion current densities of different copper-tin alloy coatings	106
4.1 Concentration of dissolving species in the electroplating baths used for producing quarternary Yellow and White Miralloys coatings	108
4.2 Electroplating duration and current density applied for multilayer deposition	109
4.3 The values of interplanar spacing (d) and preference orientation for quarternary alloy coatings	123
4.4 Thickness distribution of quarternary copper-tin-zinc-nickel coating	127
4.5 Corrosion rate of binary and quarternary Yellow and White Miralloy coatings	128
B1 Composition materials needed to prepare the solution for binary coatings	151



B2	Composition materials needed to prepare the solution for quarternary coatings	152
D1	Results of cathodic current efficiency for binary copper-tin alloy coatings	157
D2	Results of cathodic current efficiency for quarternary copper-tin-zinc-nickel alloy coatings	158
E1	The values of interplanar spacing (d) and the preference orientation for the reference	159
F1	Results of Vickers microhardness for binary copper-tin alloy coatings	160
F2	Results of Vickers microhardness for quarternary copper-tin-zinc-nickel alloy coatings	161
F3	Results of Vickers microhardness for compositionally modulated multilayer alloy coatings	161
G1	Corrosion rate of binary copper-tin alloy coatings obtained from polarization in 2 g/l H <sub>2</sub> SO <sub>4</sub> solution	162
G2	Corrosion parameters quarternary white and yellow copper-tin-zinc-nickel alloy coatings obtained from polarization in 2 g/l H <sub>2</sub> SO <sub>4</sub> solution	162
H1	Tensile properties of quarternary and multilayer alloy coatings	163

## LIST OF FIGURES

	Page
1.1 Proposed research stages for preliminary experiments	7
1.2 Proposed research stages for production of nanometer scale of Compositionally Modulated Multilayer (CMM)	9
2.1 Component of Electroplating	17
2.2 Potential–pH diagrams for Ni–H <sub>2</sub> O system at 25°C [Pourbaix, 1974]	20
2.3 Potential–pH diagrams for Sn–H <sub>2</sub> O system at 25°C [Pourbaix, 1974]	22
2.4 Plot of $\log  i $ vs $\eta$	24
2.5 A general qualitative description of the relationship between current density and potential	26
2.6 Schematic cross-section showing microroughness of cathode, at peaks (P), supply of electroactive species is relatively rapid over the short distance from the diffusion boundary, whereas at valley (V) it is too slow	27
2.7 Discharge site on a growing surface: (1) surface vacancy; (2) ledge vacancy; (3) ledge kink; (4) ledge; (5) layer nucleous	30
2.8 Growth screw dislocation with a kinked growth ledge	31
2.9 Schematic representation of layer growth (a,b) and the nucleation-coalescence mechanism (c)	32
2.10 Dependence of crystal growth mode and current density on overpotential	34
2.11 Schematic cross section (perpendicular to the substrate) of the columnar deposit	35
2.12 Polarization behavior for co-deposition of metals M <sub>1</sub> and M <sub>2</sub> . (a) M <sub>1</sub> and M <sub>2</sub> having similar E/i curves. (b) M <sub>2</sub> polarizing more than M <sub>1</sub>	39
2.13 Unit cells of the three most importance lattices	40
2.14 Schematic illustration of corrosion of coating substrate systems in the presence of pores. M, metal. (a) More noble coating on less noble substrate (galvanic corrosion). Increased corrosion of substrate material with small anodic area and large cathodic area. (b) Less noble coating on more noble substrate (anodic corrosion). Cathodic protection of substrate material, coating material dissolved, large anodic area, small cathodic area.	43

2.15	Current density vs potential curve for a typical metal electrode in neutral or acid solution. Active and passive regions are indicated with arrows. $E_{t1}$ : transpassive potential due to oxygen evolution on passive metal; $E_{t2}$ : transpassive potential which indicates passive film dissolution.	44
2.16	Potential–pH diagrams for Cu–H <sub>2</sub> O system at 25 °C [Pourbaix, 1974]	50
2.17	Potential–pH diagrams for Zn–H <sub>2</sub> O system at 25 °C [Pourbaix, 1974]	51
2.18	The current pulse electroplating of Cu/Ni multilayered composites	56
2.19	Tensile strength vs. copper layer thickness for 90%Ni-10%Cu electrodeposited multilayered	60
3.1	Set up of electrochemical cell for polarization measurement	67
3.2	Haring-Blum cell utilized for the determination of the throwing power	68
3.3	Schematic of the electroplating apparatus for binary Cu-Sn alloy coating	70
3.4	Manual mounting press model Imptech, series M 10	72
3.5	Scanning Electron Microscope (SEM) model LEO Supra 35 VP	73
3.6	Diffractionmeter Siemens D5000	75
3.7	Shimadzu micro hardness tester type M	76
3.8	Cathodic polarization curves measured at 65 °C for the electrodeposition of (i) pure copper from solution containing 5 g/l Cu(CN) <sub>2</sub> , (ii) pure tin from solution containing 45 g/l Na <sub>2</sub> SnO <sub>3</sub> and (iii) copper-tin alloy from solution containing 5 g/l CuCN <sub>2</sub> , 45 g/l Na <sub>2</sub> SnO <sub>3</sub> . Each solution contained 12 g/l NaOH and 25 g/l NaCN	79
3.9	Cathodic polarization curves measured at 65 °C for the electrodeposition of (i) pure copper from solution containing 10 g/l Cu(CN) <sub>2</sub> , (ii) pure tin from solution containing 45 g/l Na <sub>2</sub> SnO <sub>3</sub> and (iii) copper-tin alloy from solution containing 10 g/l CuCN <sub>2</sub> , 45 g/l Na <sub>2</sub> SnO <sub>3</sub> . Each solution contained 12 g/l NaOH and 25 g/l NaCN	79
3.10	Cathodic polarization curves measured at 65 °C for the electrodeposition of (i) pure copper from solution containing 15 g/l Cu(CN) <sub>2</sub> , (ii) pure tin from solution containing 45 g/l Na <sub>2</sub> SnO <sub>3</sub> and (iii) copper-tin alloy from solution containing 15 g/l CuCN <sub>2</sub> , 45 g/l Na <sub>2</sub> SnO <sub>3</sub> . Each solution contained 12 g/l NaOH and 25 g/l NaCN	80

3.11	Cathodic polarization curves measured at 65 °C for the electrodeposition of (i) pure copper from solution containing 20 g/l $\text{Cu}(\text{CN})_2$ , (ii) pure tin from solution containing 45 g/l $\text{Na}_2\text{SnO}_3$ and (iii) copper-tin alloy from solution containing 20 g/l $\text{CuCN}_2$ , 45 g/l $\text{Na}_2\text{SnO}_3$ . Each solution contained 12 g/l NaOH and 25 g/l NaCN	80
3.12	Experimental polarization curves measured at 65 °C for the electrodeposition of copper-tin alloys from bath containing 45 g/l $\text{Na}_2\text{SnO}_3$ , 25 g/l NaCN, 12 g/l NaOH, and different concentrations of $\text{Cu}(\text{CN})_2$ : (i) 5 g/l, (ii) 10 g/l, (iii) 15 g/l, (iv) 20 g/l	82
3.13	Cathodic polarization curves of coatings produced during first polarization in the bath solution containing 10 g/l $\text{Cu}(\text{CN})_2$ , 45 g/l $\text{Na}_2\text{SnO}_3$ , 2 g/l NaOH and 25 g/l NaCN at temperature 65°C	83
3.14	Cathodic polarization curves of alloy measured at different temperature 60 °C, 65 °C, and 70 °C in the bath solution containing 20 g/l $\text{Cu}(\text{CN})_2$ , 45 g/l $\text{Na}_2\text{SnO}_3$ , 12 g/l NaOH and 25 g/l NaCN	83
3.15	Copper concentration obtained from EDX analysis on the inner, middle and outer parts of the cross section of coatings developed from (a) bath I; (b) bath II; (c) bath III and (d) bath IV	86
3.16	The cross section of a Cu-Sn alloy coating developed in electroplating bath I at current density 5 mA/cm <sup>2</sup> and its representative EDX spectra for the inner layer (b), middle layer (c) and outer layer (d)	87
3.17	Cathodic current efficiency of the binary copper-tin from different bath and current density	88
3.18	X-ray diffraction patterns of binary coatings obtained from (a) bath I, current density 4.88 mA/cm <sup>2</sup> ; (b) bath II, current density 5.00 mA/cm <sup>2</sup> and (c) bath II, current density 18.36 mA/cm <sup>2</sup>	90
3.19	X-ray diffraction patterns of binary coatings obtained from (a) bath III, current density 5.00 mA/cm <sup>2</sup> ; (b) bath III, current density 9.93 mA/cm <sup>2</sup> ; (c) bath III, current density 18.76 mA/cm <sup>2</sup> ; (d) bath IV, current density 5.05 mA/cm <sup>2</sup> and (e) bath IV, current density 19.76 mA/cm <sup>2</sup>	91
3.20	Phase diagram of copper-tin (Cu-Sn)	93
3.21	SEM micrographs of the copper-tin electrodeposits from bath I at current densities (a) 4.88 mA/cm <sup>2</sup> ; (b) 9.52 mA/cm <sup>2</sup> and (c) 18.76 mA/cm <sup>2</sup>	96
3.22	SEM micrographs of the copper-tin electrodeposits from bath II at current densities (a) 5.00 mA/cm <sup>2</sup> ; (b) 10.34 mA/cm <sup>2</sup> and (c) 18.37 mA/cm <sup>2</sup>	97
3.23	SEM micrographs of the copper-tin electrodeposits from bath III at current densities (a) 5.00 mA/cm <sup>2</sup> ; (b) 9.93 mA/cm <sup>2</sup> ; (c) 18.76 mA/cm <sup>2</sup>	98

3.24	SEM micrographs of the copper-tin electrodeposits from bath IV at current densities (a) 5.05 mA/cm <sup>2</sup> ; (b) 10.09 mA/cm <sup>2</sup> and (c) 19.76 mA/cm <sup>2</sup>	99
3.25	Thickness uniformity of binary copper-tin coating produced in electroplating bath IV at current density 5 mA/cm <sup>2</sup>	100
3.26	Cross sectional of the substrates-coating system at higher magnification (a) taken at the left side and (b) taken at the right side of coating presented in Figure 3.25	100
3.27	Scanning electron microscope of the diamond indentation tip the coating produced from the bath III, current density 5 mA/cm <sup>2</sup>	101
3.28	Average microhardness of coatings developed in different electroplating baths at different current densities	101
3.29	Polarization curves of mild steel, pure copper and tin in 2 g/l solution H <sub>2</sub> SO <sub>4</sub> at 25 °C	102
3.30	Polarization curves obtained in 2 g/l solution H <sub>2</sub> SO <sub>4</sub> at 25 °C for binary Cu-Sn alloy coatings developed in the electroplating bath I	104
3.31	Polarization curves obtained in 2 g/l solution H <sub>2</sub> SO <sub>4</sub> at 25 °C for binary Cu-Sn alloy coatings developed in the electroplating bath II	104
3.32	Polarization curves obtained in 2 g/l solution H <sub>2</sub> SO <sub>4</sub> at 25 °C for binary Cu-Sn alloy coatings developed in the electroplating bath III	105
3.33	Polarization curves obtained in 2 g/l solution H <sub>2</sub> SO <sub>4</sub> at 25 °C for binary Cu-Sn alloy coatings developed in the electroplating bath IV	105
4.1	Schematic of the electroplating apparatus for quaternary Cu-Sn-Zn-Ni alloy coatings	107
4.2	Procedure for CMM electroplating	110
4.3	Shape and dimension of rectangular tension test specimen	113
4.4	Macrograph of coated test specimens	114
4.5	A schematically stress-strain curve showing elastic and plastic regions	115
4.6	Composition of plating was obtained from a few points across the plating using EDS analysis from bath solution V	118
4.7	Composition of plating was obtained from a few points across the plating using EDS analysis from bath solution VI	118
4.8	Composition of coating developed in electroplating bath V at different current densities	119

4.9	Composition of coating developed in electroplating bath VI at different current densities	119
4.10	Cathodic current efficiency of the quarternary copper-tin-zinc-nickel alloy electroplating in different electroplating baths and current densities	121
4.11	X-ray diffraction patterns of quarternary coatings obtained from (a) bath V, current density 10 mA/cm <sup>2</sup> ; (b) bath VI, current density 20 mA/cm <sup>2</sup>	122
4.12	SEM micrographs of the copper-tin-zinc-nickel electrodeposits from bath V at current densities (a) 5mA/cm <sup>2</sup> ; (b) 10 mA/cm <sup>2</sup> ; (c) 20 mA/cm <sup>2</sup> ; (d) 25 mA/cm <sup>2</sup> and (e) 30 mA/cm <sup>2</sup>	124
4.13	SEM micrographs of the copper-tin-zinc-nickel electrodeposits from bath solution VI at current densities (a) 5mA/cm <sup>2</sup> ; (b) 10 mA/cm <sup>2</sup> ; (c) 20 mA/cm <sup>2</sup> ; (d) 25 mA/cm <sup>2</sup> and (e) 30 mA/cm <sup>2</sup>	125
4.14	Thickness uniformity of a deposited quarternary copper-tin-zinc-nickel coating produced from bath VI, current density 20 mA/cm <sup>2</sup>	127
4.15	SEM image of coating cross section produced in electroplating bath VI at current density of 20 mA/cm <sup>2</sup>	127
4.16	Polarization behavior of quarternary Yellow and White Miralloy	128
4.17	SEM micrographs of the white/yellow multilayer coating with thickness layer 1 $\mu$ m (a) view at low magnification (600 X), (b) view at high magnification (10000 X)	129
4.18	Back scattered image of cross-sectional CMM deposits with sub-layer thickness of 1 $\mu$ m, (a) at low magnification (600 X), (b) at high magnification (3000 X)	130
4.19	EDX spectra back-scattered electron images for CMM deposits with sub-layer thickness of 1 $\mu$ m	131
4.20	The secondary and back-scattered electron images of White and Yellow miralloy multilayer with thickness layer 500 nm	132
4.21	The secondary electron images of White and Yellow Miralloy multilayers with thickness layer (a) 310 nm; (b) 107.9 nm; (c) 46.82 nm and (d) 24.66 nm	133
4.22	Microhardness of quarternary Yellow and White Miralloy and CMM specimens	134
4.23	Vickers microhardness of Yellow-White multilayer as a function of bilayer thickness d	135
4.24	Comparison of stress-strain curves of white-yellow multilayers with that of mild steel, white and yellow single layer	137

4.25	The fracture surface of the as-deposited single layer (a) Yellow Miralloy and (b) White Miralloy	138
4.26	The fracture surface of the as-deposited multilayer White/Yellow Miralloy with layer thickness of (a) 1000 nm; (b) 500 nm; (c) 300 nm; (d) 100 nm; (e) 50 nm; and (f) 20 nm	139
A1	Potential–pH diagrams for Cu–CN–H <sub>2</sub> O system at 25 °C and the activities of all solute species of (a) 1; (b) 10 <sup>-2</sup> ; (c) 10 <sup>-4</sup> ; (d) 10 <sup>-6</sup> considering Cu(OH) <sub>2</sub> as a stable species and using the data in Table 3. HCNO, CNO <sup>-</sup> and (CN) <sub>2</sub> are not considered	149
C1	Phase diagram of copper-zinc (Cu-Zn)	153

## LIST OF ABBREVIATION

at.%	: Atom percentage
ASM	: American society of metals
ASTM	: American standards for testing of materials
BCC	: Body center cubic
BSE	: Back scattered electron
CCE	: Cathodic current efficiency
CMM	: Compositionally modulated multilayer
Cu-Sn	: Copper Tin
CR	: Corrosion rate
DC	: Direct current
EDX	: Energy dispersive x-ray spectroscopy
FCC	: Face center cubic
FESEM	: Field Emission scanning electron microscopy
HER	: Hydrogen evolution reaction
ICCD	: International center diffraction data
Mpa	: Mega pascal
nm	: Nanometer
SEM	: Scanning electron microscope
WE	: Working electrode
wt.%	: Weight percentage
TP	: Throwing power
XRD	: X-ray diffraction
μm	: Micrometer



## LIST OF SYMBOLS

<b>a</b>	: Activity
<b>A</b>	: Surface area of electrode
<b><math>\alpha</math></b>	: Transfer coefficient
<b><math>\beta</math></b>	: Symmetry factor
<b><math>C^\circ</math></b>	: Bulk concentration
<b><math>\delta</math></b>	: Diffusion coefficient
<b>d</b>	: Interplanar spacing
<b>E</b>	: Electrode potential
<b><math>E^\circ</math></b>	: Standard electrode potential
<b><math>\eta</math></b>	: Overpotential
<b>F</b>	: Faraday's constant
<b>i</b>	: Current density
<b><math>i_o</math></b>	: Exchange current density
<b><math>i_L</math></b>	: Limiting current density
<b><math>J_T</math></b>	: Total flux of ion
<b><math>J_c</math></b>	: Convection flux
<b><math>J_D</math></b>	: Diffusion flux
<b><math>J_M</math></b>	: Migration flux
<b>K</b>	: Ratio of distances between the anode and the two cathodes
<b>M</b>	: Molecule mass
<b><math>\rho</math></b>	: Density
<b>n</b>	: Number of electron
<b>T</b>	: Temperature
<b>t</b>	: Time
<b><math>t_+</math></b>	: Transfer number

**$\theta$**  : Angle

**M** : Ratio of weights of metal deposited for two cathodes

# **PENYADURAN ALOI Cu-Sn DAN LAPISAN BERBILANG DENGAN KOMPOSISI TERMODULAT ALLOY Cu-Sn-Zn-Ni PADA SUBSTRAT KELULI LEMBUT**

## **ABSTRAK**

Dua siri eksperimen elektrosaduran telah dijalankan pada substrat keluli lembut pada suhu 65 °C dalam beberapa mandian elektrosaduran di bawah ketumpatan arus konstan yang berlainan. Tujuan eksperimen siri pertama adalah untuk mengkaji perilaku proses pemendapan elektro Cu dan Sn dari beberapa mandian sianida beralkali dan untuk memperoleh syarat elektrosaduran supaya dapat menghasilkan saduran Miralloys perduaan kuning dan putih. Eksperimen siri kedua melibatkan kajian eksperimen lapisan berbilang dengan komposisi termodulat yang mengandungi lapisan nano kuarterner Miralloy kuning dan putih secara berselang-seli dengan menggunakan teknik dua mandian. Kinetik dan sifat elektrosaduran aloi Cu-Sn telah dikaji melalui pengukuran sifat polarisasi katodik keduanya dalam mandian elektrosaduran yang berlainan. Pengaruh komposisi mandian dan ketumpatan arus pada komposisi dan sifat perduaan saduran Cu-Sn aloi pada substrat keluli lembut telah dilakukan menggunakan mandian elektrosaduran. Keseragaman saduran yang dihasilkan dalam eksperimen ini diperiksa di bawah FE-SEM, sementara keseragaman komposisi saduran dan fasa-fasa yang ada dalam saduran masing-masing dikaji dengan EDX dan XRD. Saduran aloi perduaan Cu-Sn dan kuarterner Cu-Sn-Zn-Ni khususnya Miralloy kuning dan putih yang tumpat, merekat, berpermukaan halus, dan seragam dapat dihasilkan pada substrat keluli lembut dengan kadar laju yang tinggi. Penambahan zink dan nikel dalam saduran tidak banyak merubah sifat-sifat kimia dan mekanik saduran. Pembentukan saduran lapisan berbilang dengan komposisi termodulat yang mengandungi lapisan berbilang yang berskala nano telah meningkatkan kekerasan mikro saduran. Pengenapan lapisan saduran berbilang dengan ketebalan lapisan < 300 nm adalah sangat berarti. Hubungan antara ketebalan

dua lapisan ( $d^{-1/2}, (\mu\text{m})$ ) dan kekerasan mikro saduran (HV) didapat  $HV = 17.37d^{-1/2} + 602.66$ . Kekerasan yang paling tinggi dari saduran lapisan termodulat kerencaman berbilang yang diperoleh dari eksperimen ini adalah 689.62 HV dan ini dihasilkan dari saduran lapis berbilang yang mengandung lapis Miralloy kuning dan putih yang berselang-seli dengan ketebalan sub-lapisan 20-30 nm. Dari eksperimen ini dapat dinyatakan bahawa pembentukan saduran aloi Cu-Sn atau Cu-Sn-Zn-Ni terutama saduran lapisan termodulat memungkinkan aplikasi saduran timah untuk industri automotif.

# **ELECTROPLATING OF Cu-Sn ALLOYS AND COMPOSITIONALLY MODULATED MULTILAYERS OF Cu-Sn-Zn-Ni ALLOYS ON MILD STEEL SUBSTRATE**

## **ABSTRACT**

Two series of electroplating experiments have been carried out onto mild steel substrate at 65 °C in several electroplating baths under different constant applied current densities. The objectives of the first series of experiments are to understand the behavior of electrodeposition of Cu and Sn in the several alkaline cyanide baths and to explore the electroplating conditions which are appropriate for fabricating binary Yellow and White Miralloys coatings. The second series of experiments deals with an experimental study on electroplating of Compositionally Modulated Multilayer (CMM) consisting of multiple alternate nano-layers of quaternary Yellow and White Miralloys using dual bath technique (DBT). The kinetics and electrodeposition behavior of Cu-Sn alloys have been assessed by measuring their cathodic polarization behavior in selected electroplating baths. The influence of bath composition combined with current density to the compositions and properties of binary Cu-Sn and quaternary Cu-Sn-Zn-Ni alloys coatings deposited onto mild steel substrate have been studied in several electroplating baths. The uniformity of the coatings developed in this experiment is examined under FE-SEM, while the compositional uniformity of coating and phases present in the coating are assessed by EDX and XRD respectively. Dense, adherent, smooth and uniform binary Cu-Sn and quaternary Cu-Sn-Zn-Ni alloys coatings especially Yellow and White Miralloys, can be deposited with relatively high deposition rate. Introducing zinc and nickel into the coating does not significantly alter their chemical and mechanical properties. Formation CMM coatings has significantly increased the micro-hardness of the coatings. However, fabrication of multilayer coatings with individual layer thickness < 300 nm are essential. The relationship between the bilayers thickness ( $d^{-1/2}$ , (μm)) and coating micro hardness (HV) has been

formulated as  $HV = 17.37d^{-1/2} + 602.66$ . The highest hardness of CMM coating obtained from this experiment is 689.62 HV and this is achieved by fabricating CMM coating consisting of multiple alternate thin layers of Yellow and White Miralloys with individual layer thickness of 20-30 nm. This experiment confirms that the formation of Cu-Sn or Cu-Sn-Zn-Ni alloys coatings especially CMM coating have made the application of tin for automotive industries feasible.

## **CHAPTER 1 INTRODUCTION**

### **1.1 Research Background**

Tin is one of the first metals mined and has been recognized previously as an important metal in industry. The largest tin mines are mostly in Asia. The most important ore-supplying countries in the Asia are Indonesia, Malaysia and followed by China [Habashi, 1997; Malaysian Chamber of Mines, 2006] and only Indonesia and China after about 1994. Currently, the Malaysian Smelting Corporation (MSC) group is one of the largest integrated producers of tin metal and tin-based products in the world. In 2004, the group contributed about 18% of the world's tin production with a combined production of 57,270 tons of tin metal from the group's smelting operations in Malaysia and Indonesia (MSC Annual Report, 2004). Most of the tin consumption in the world is for producing tin solders, tin coatings, tin compounds and alloys containing tin. Besides tin metal exhibits unique properties such as low melting point and resistant to corrosion, tin has also recognized as a green metal (non toxic metal) and therefore tin is still used as a base metal for producing lead free solders and it also considered as a proper metal for substituting lead such as for fishing tackles and shot gun bullets. In ASEAN countries for instance, the major consumption of tin metal is for producing tin solders, tin cans and pewter. Even though tin is an important metal in industry, the annual (demand) is still small compared to those of many other metals. It has been reported that the world production and consumption of tin have not really grown in the past 20 years, due mainly to the substitution of tin by plastic, paper or aluminum in the manufacture of cans and other containers, such as plastic tubes for toothpaste and ointments. Consequently, attempts should be made by Tin Mining and Tin Smelting Companies to increase or at least to maintain the world tin consumption. This is done by increasing the role of tin in various applications. One of the possibilities to increase

the world tin consumption which is in consideration recently, is to increase the role of tin in electroplating industries.

Electroplating is widely used for production of new materials that require specific mechanical, chemical and physical properties. This technique has demonstrated to be very convenient because of its simplicity and low cost in comparison with the other method such as sputtering and vapor deposition. Pure tin is non-toxic, can be electrodeposited as an extremely bright, white and lustrous deposit. It has excellent resistance to corrosion and easily to be soldered. As mentioned previously, it is being applied to produce tin cans for food packaging. However, pure tin is soft and is not practical to be used as coated material for automotive applications. While the hardness of alloys coatings such as White Miralloy (55%Cu-45%Sn or 55%Cu-30%Sn-15%Zn) and Yellow Miralloy (80%Cu-17.5%Sn-2.5%Zn, 80%Cu-15%Sn-5%Zn or 85%Cu-15%Sn) are respectively 550 HV and 400 HV. These coating layers are extremely abrasion resistant and are suitable for automotive application. The coatings also exhibit other interesting characteristics such as low surface tension, good sliding ability, high hardness, sufficient ductility, solder ability, low porosity and/or resistance to corrosion depending on their composition. Such properties have led to these coating being widely used in industries. For example, because of White Miralloys exhibit an acceptable contact resistance, it may be used for coating electric connectors. More over, worn machine parts can be re-electroplated by these alloys to extend their service life. These may lead to a decrease in the cost of the parts.

Recently, it has been reported that electroplating of Cu-Sn alloys can be successfully done in laboratories using non cyanide solution e.g. in acid sulfate solution [Survila, et al. 2004]. Even though co-deposition of such alloys can be done using non-cyanide baths, most of the industrial tin alloys plating use cyanide solutions because of the high quality requirement of the coating [Picincu, et al., 2001]. Electrocodeposition in



cyanide bath will produced adherent, smooth and uniform coating on both planar and non planar substrates. Moreover quarternary alloys (e.g. an alloy which contains Cu 50 %wt, Sn 32 %wt, Zn 17 %wt and Ni 1%wt) can be easily electrocodeposited from cyanide baths [Helton et. al, 1989]. Cyanide is deemed typical of complexing agents that have been used for long time in providing stable solution. It is still used intensively in industries such as in gold extraction plants and in electroplating industries as “strike” solution. However, extra care has to be performed to avoid fatal accident and to eliminate environmental problem especially during disposal of cyanide. Despite the fact that cyanide systems are the most toxic electrolytes known, the technology of waste disposal treatment on them is well established and has been implemented in industries for many years.

Multilayers especially compositionally modulated multilayer (CMM) coatings, consisting of multiple alternate thin layers of alloys, have received increasing attention recently because of their unique properties. These materials comprised of alternating layers of different metals and /or alloys are expected to exhibit unusual and enhanced electrical, optical, magnetic and mechanical properties when the sublayer thickness is confined to the nanometer scale [Miyake, et al. 2001]. The properties of multilayered systems depend on bilayer thickness, global thickness and good multilayer formation [Gomez, et al. 2003]. However, most of the studies of CMM coatings have been reported for Cu/Ni, Cu/Co-Ni, Cu/Ni-Fe, Au/Co, Pt/Co etc. [Haseeb, et al. 1994; Kanani, 2004]. So far, there is no research has been reported on the production of CMM coatings consisting of multiple alternate thin layers of Yellow and White Miralloys or White Miralloy with another metal such as gold, silver, platinum, palladium, etc, in order to increase the electric conductivity of the coatings.

## **1.2 Research Objectives**

The research reported in this thesis relates to a study of electro-codeposition of Cu-Sn and Cu-Sn-Zn-Ni alloys on mild steel substrate from several cyanide baths. Its main objective is to find electroplating conditions that are suitable for producing binary and quaternary Yellow and White Mirralloys. It is also proposed to extend the research of previous workers [e.g. Helton et. al, 1989; Picincu et al., 2001] by investigating the possibility to produce CMM coatings consist of multiple alternate thin layers of Yellow and White Miralloys using a dual baths technique. These multilayer coatings were expected to be harder than that of White Miralloy, but it is still exhibited suitable resistant to corrosion.

The study has been focused on the production of coatings and most of characterization measurements have been proposed to collect additional information which will be used to obtain range of electroplating conditions in which adherent, smooth and uniform Yellow and White Miralloys as well as CMM coating can be produced. It consists of two series of experiments namely Preliminary Experiment and Production of CMM Consisting of Multiple Alternate Nano-Layers of Yellow and White Miralloys.

The scopes of the research are as follows:

### **Part A. Preliminary Experiment**

The possibility to electro-codeposition of Cu-Sn alloy coatings onto mild steel substrate in cyanide baths is studied. The compositions of these plating baths are adopted from established Cu-Sn alloys plating composition cited in electroplating texts [Gabe, 1974; Pletcher et al., 1990]. All of the electroplating solutions utilized in this experiment contain saturated  $\text{Na}_2\text{SnO}_3$ . Factors that influence the composition and properties of binary alloys which are deposited from these plating solutions are observed. The

results are used to select the composition of plating baths for depositing quarternary Cu-Sn-Zn-Ni alloys and compositionally modulated multilayers consisted of multiple alternate quarternary Yellow and White Miralloys layers on a mild steel substrate. The research of this part will include :

1. Measurement cathodic polarization behavior of Cu, Sn and Cu-Sn from selected cyanide solutions.
2. A study on the influence of current density on the composition, phases formed and uniformity of Cu-Sn deposits produced from several electroplating bath compositions at 65 °C.
3. An assessment on the influence of chemical composition of coatings to their micro-hardness and corrosion resistance in 2 g/l H<sub>2</sub>SO<sub>4</sub> solution at ambient temperature.

## **Part B. Production of Compositionally Modulated Multilayer Consisting of Multiple Alternate Nano-Layers of Quarternary Yellow and White Miralloys**

Since electroplating of quarternary Cu-Sn-Zn-Ni alloys may produce brighter coatings and multilayers coating is expected to possess outstanding coating properties, the main objective of this part is to produce multilayer coating consisted of multiple alternate quarternary Yellow and White Miralloys layers. Consequently, the experiment must be initiated with the observation of factors that influence the composition and properties of quarternary alloys deposited from designated prepared plating solutions. Hence, the main research activities of this part are:

1. Exploring the proper electroplating conditions which are appropriate for fabricating quarternary Yellow and White Miralloys onto mild steel substrate.
2. Investigating the possibility of production compositionally modulated multilayer consisting of multiple alternate nano layers of Yellow and White Miralloys on mild steel substrate using a dual baths method.

3. Investigating the influence of the present of Zn and Ni in the coating to the corrosion resistant of Yellow and White Miralloys.

### **1.3 Research Methodology**

Research activities are conducted following the flow charts presented in Figure 1.1 and 1.2. It is initiated by selecting the electroplating system that is suitable for binary and quaternary Cu-Sn-Zn-Ni deposition. High throwing power alkaline cyanide baths is chosen and its throwing power is remeasured using a conventional test method in a Haring Blum cell. The polarization curves of Cu, Sn and Cu-Sn alloy depositions is further measured, both on steel and coated steel specimens. This will give information the kinetics of Cu, Sn and Cu-Sn alloy deposition. Since Cu and Sn depositions might not occur with the same rate during alloy electroplating, the composition of the coating is expected to be influenced by deposition potential/current density which is a function of total current density and the concentration of electroactive species in the electroplating bath. Consequently study the influence of bath composition and current density to the chemical composition of binary Cu-Sn coating produced is necessary to be considered. The physical and chemical properties of the coatings are further characterized using SEM and EDX, micro hardness testing machine and potentiostat. This preliminary experiment is followed by investigating the influence of current density to the chemical composition of quaternary Cu-Sn-Zn-Ni coatings developed in selected electroplating baths for depositing Yellow and White Miralloys. The coatings produced are then subjected to be characterized with the same characterization procedures applied for binary coatings. The best electroplating bath compositions and electroplating conditions for depositing quaternary Yellow and White Miralloys are explored and they will be utilized for producing nanometer scale compositionally modulated multilayers using a dual baths technique.

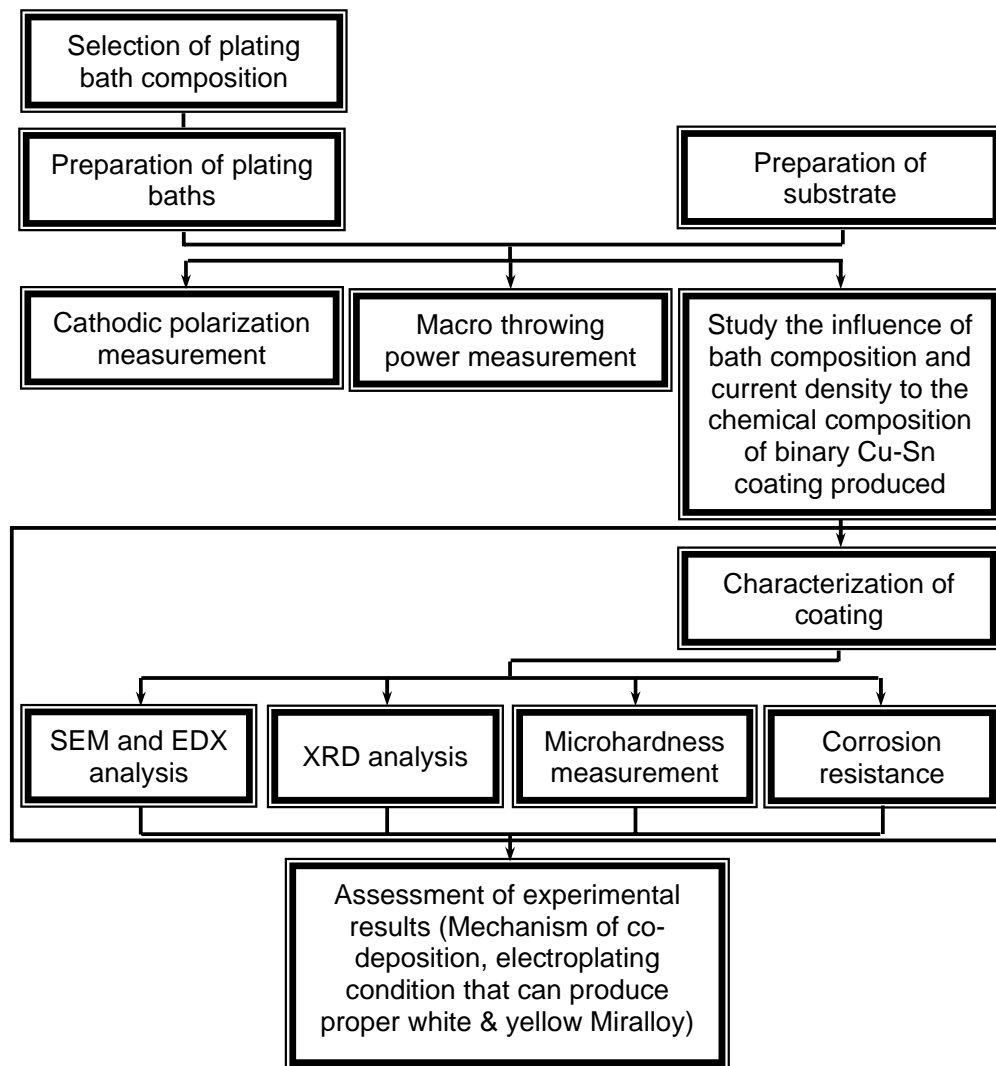


Figure 1.1: Proposed research stages for preliminary experiments

## Plating Baths Selection

In electrodeposition of alloys, the electrolyte and deposition conditions are chosen so that deposits have uniform composition and properties over the course of the deposition process. Based on potential-pH equilibrium diagrams for the systems Cu-H<sub>2</sub>O, Sn-H<sub>2</sub>O, Zn-H<sub>2</sub>O and Ni-H<sub>2</sub>O which are respectively presented in Figure 2.16, 2.3, 2.17 and 2.2, electroplating can be done either in acid or in alkaline solutions. In acid solution electroplating may be conducted by reducing simple cations (e.g. Cu<sup>2+</sup>, Sn<sup>2+</sup>,

$\text{Zn}^{2+}$  or  $\text{Ni}^{2+}$ ) while in alkaline deposition must be conducted by reducing complex anions. Electroplating of metal/alloy from simple cation onto non planar metal substrates tends to produce a non-uniform coating because local deposition current density at location close to anode will be significantly higher than that at locations far from the anode. Basically ternary Cu-Sn-Ni alloys can be co-deposit during electroplating and zinc is not expected to be deposited simultaneously with the alloy because its deposition potential is too low. Thereby the utilization of alkaline cyanide solution has been selected for producing quaternary Cu-Sn-Ni-Zn coating for this experiment.

More uniform deposit can be obtained for the electroplating which is influenced by mass transfer of cation toward the cathode especially at locations closer to anode. In contrast electroplating from complex anion in alkaline solution will tends to produce more uniform coating because the complex anion will migrate away from the cathode and the rate of migration will be higher at locations closer to anode. More over electroplating from alkaline solution will have advantages such as: (1) electroplating bath has higher covering power; (2) more uniform thickness coating can be formed on non planar substrate; (3) solution is not very corrosive compared to acid solution; (4) less hydrogen evolution and thus coating will be less brittle compared to that produced in acid solution. It should be noted that no Cu-Sn-Ni-Zn alloy deposition will occur except the deposition potential of copper can be lower close to Sn, Zn and Ni. Based on the potential-pH diagram Cu-CN-H<sub>2</sub>O system (Appendix A) [Lu et. al. 2002], the deposition potential of copper from alkaline cyanide bath can be suppressed as low as the deposition potential for zinc and therefore codeposition of Cu, Sn, Zn and Ni can be done simultaneously in this plating bath.

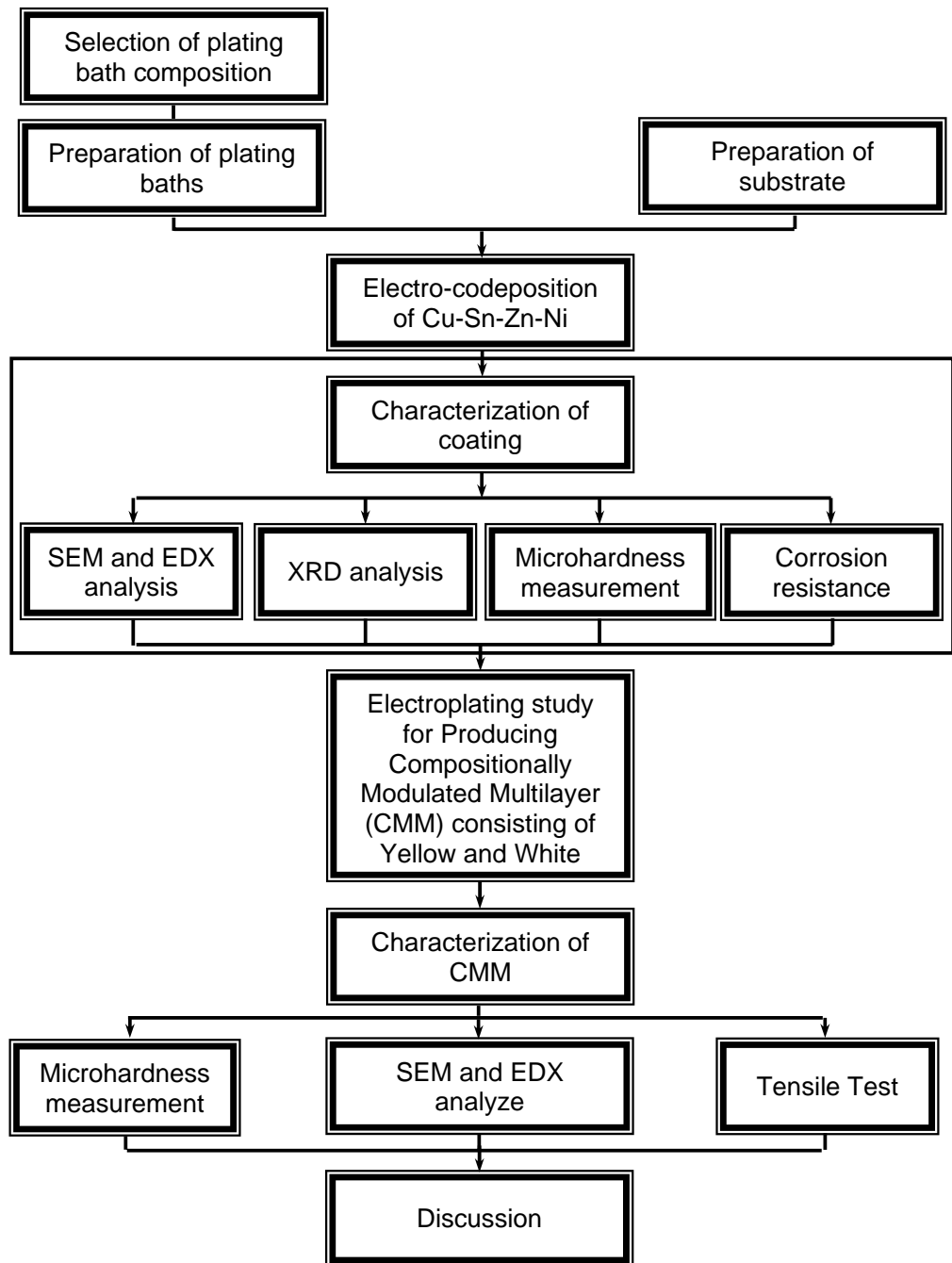


Figure 1.2: Proposed research stages for production of Compositionally Modulated Multilayer (CMM) coatings consisted of nanometer scale of Yellow and White miralloys.

### Selection of Substrate

There are at least two reasons why mild steel is used as a substrate in this alloy plating experiment;

- (1) One of the aims of the electroplating experiment is to prepare alloy plating for automotive application which most substrate is steel including mild steel,
- (2) Alloy plating is more difficult to be implemented on steel rather than on copper because the equilibrium potential of steel is significantly lower than that of copper. Therefore, if alloy plating can be successfully done on mild steel, it will be successfully conducted on copper e.g. for plating electric connector.

### **Throwing power measurement**

Throwing (macrothrowing) power of the electroplating bath is determined experimentally using a small electroplating cell of special geometrical shape (Haring-Blum). Two cathodes are placed at markedly different distances from a single anode and electroplating is carried out. The throwing power is calculated using the following equation

$$\% \text{ throwing power} = \frac{100(K - M)}{K + M - 2} \quad (1.3)$$

where K and M are ratios of distance from the anode and weights of metal deposited for two cathodes respectively. ( $K = X_2 / X_1$ ,  $M = W_1 / W_2$ )

### **Polarization measurement**

An alloy deposition process is more complex than that for single metal deposition. However, an examination of partial polarization curves from alloy deposition and from single metal deposition under similar condition can help to understand the mechanism of deposition process of copper-tin alloys. Cathodic polarization behavior for single metals and alloy deposition processes will be discussed and used to gain qualitative information on the mass transport and kinetic aspects of binary and quaternary copper-tin alloys deposition. All of polarization curves are measured in an electrochemical cell consisted of three electrodes and test solution as its electrolyte. The measurements are conducted in a slightly stirred solution open to air using a



Gamry's potentiostat with the scanning rate of 5 mV/second. Saturated copper sulphate and graphite electrodes are employed respectively for reference and counter electrodes.

### **The influence of the common variables in alloy plating**

The independent variables which are current density, agitation, temperature, pH, and concentration of bath constituents, influence the ratio in which two or more metals are co-deposited, the physical and chemical characteristics of the coatings, and the rate of deposition. An appreciable change in any one variable may require an appreciable and compensating change in another variable or combination of variables in order to maintain a given plate composition or physical properties, each variable can be considered with regard to its general effect. In this experiment agitation and temperature are maintained constant. The concentration of  $\text{Cu}(\text{CN})_2$  will be varied between 5 and 20 g/l in the bath solution while the concentration of  $\text{Na}_2\text{SnO}_3$ , NaCN and NaOH are fixed on 45, 25 and 12 g/l respectively. The duration time of deposition (t) are proposed to be 8.5 hours (30600 seconds) for current density 5  $\text{mA}/\text{cm}^2$ , 3.5 hours (12600 seconds) for current density 10  $\text{mA}/\text{cm}^2$  and 94 minutes (5640 seconds) for 20  $\text{mA}/\text{cm}^2$ . The composition of electrolyte baths for quaternary deposition of White and Yellow Miralloys respectively are 20 g/l  $\text{Cu}(\text{CN})_2$ , 45 g/l  $\text{Na}_2\text{SnO}_3$ , 1 g/l ZnO, 0.03 g/l Nickel acetate, 25 g/l NaCN, and 12 g/l NaOH; and 40 g/l  $\text{Cu}(\text{CN})_2$ , 45 g/l  $\text{Na}_2\text{SnO}_3$ , 0.25 g/l ZnO, 0.02 g/l Nickel acetate, 25 g/l NaCN, and 12 g/l NaOH. Zinc and nickel are co-deposited together with Cu and Sn to promote the development of corrosion resistant, bright and untarnished coatings. Nickel is added into the electroplating bath to enhance the inclusion of tin within the plate alloy.

The cathodic current efficiency ( $\eta$ ) is calculated using the following equation

$$\text{Cathodic current efficiency} = \frac{\Delta w}{w_t} \times 100 \% \quad (1.4)$$

and the theoretical weight of electrodeposited alloy is expressed in term of Faraday's laws of electrolysis as follows;

$$w_t(1) = \left[ \frac{M_{Cu} \times i_{Cu} \times A \times t}{n_{Cu} \times F} \right] + \left[ \frac{M_{Sn} \times i_{Sn} \times A \times t}{n_{Sn} \times F} \right]$$

(1.5)

$$w_t(2) = \left[ \frac{M_{Cu} \times i_{Cu} \times A \times t}{n_{Cu} \times F} \right] + \left[ \frac{M_{Sn} \times i_{Sn} \times A \times t}{n_{Sn} \times F} \right] + \left[ \frac{M_{Zn} \times i_{Zn} \times A \times t}{n_{Zn} \times F} \right] + \left[ \frac{M_{Ni} \times i_{Ni} \times A \times t}{n_{Ni} \times F} \right]$$

(1.6)

where,  $\Delta w$  is the weight of electrodeposited alloy (gram),  $w_t$  is the theoretical weight of electrodeposited alloys (1) is indicated for binary and (2) for quaternary (gram),  $M_{Cu}$ ,  $M_{Sn}$ ,  $M_{Zn}$  and  $M_{Ni}$  are respectively the molecule mass of copper, tin, zinc and nickel (gram/mol),  $i_{Cu}$ ,  $i_{Sn}$ ,  $i_{Zn}$  and  $i_{Ni}$  are respectively the partial current densities of copper, tin, zinc and nickel (Ampere/cm<sup>2</sup>),  $A$  is the surface area of electrode (cm<sup>2</sup>),  $t$  is the duration of deposition process (second),  $n_{Cu}$ ,  $n_{Sn}$ ,  $n_{Zn}$  and  $n_{Ni}$  are the numbers of moles electron needed to reduce a unit mole of  $CuCN_2^-$ ,  $Sn(OH)_6^-$ ,  $Zn(CN_4)^-$  and  $Ni^{2+}$  ions (these are equal to 1, 4, 2 and 2, respectively), and  $F$  is the Faraday's constant (Ampere. sec. mol<sup>-1</sup>).

### Microhardness measurement

Hardness measurements are performed on polished cross section specimens at room temperature in accordance with ASTM standard E-384 [1999].

### Corrosion resistant measurement

Study of the corrosion resistance of coatings is performed by assessing their polarization behavior in relatively aggressive solution. For this study, coatings with an

exposed surface area of approximately  $1 \text{ cm}^2$  are prepared. The anodic polarization measurements are done in 2 g/l  $\text{H}_2\text{SO}_4$  solution at room temperature using the same potentiostat used for cathodic polarization measurement of electrodeposition process. The measurement method is adopted from that recommended by ASTM standard G-5. The corrosion rates of coating specimens are determined their cathodic and anodic polarization curves, while the tendencies to become passive are evaluated with respect to their anodic polarization behavior.

### **Electroplating study for producing Compositionally Modulated Multilayer (CMM) coatings**

Electrodeposition of compositionally modulated multilayers (CMM) coatings consisting of multiple alternate thin layers of Yellow and White Miralloys on a mild steel substrate is carried out using the dual baths technique. The series of experiments that we have conducted earlier suggested that the best solutions for depositing Yellow and White Miralloys are the electroplating bath containing 40 g/l  $\text{Cu}(\text{CN})_2$ , 45 g/l  $\text{Na}_2\text{SnO}_3$ , 12 g/l NaOH, 25 g/l NaCN, 0.25 g/l ZnO and 0.02 g/l  $\text{Ni}(\text{CH}_3\text{COO})_2$  and that containing 20 g/l  $\text{Cu}(\text{CN})_2$ , 45 g/l  $\text{Na}_2\text{SnO}_3$ , 12 g/l NaOH, 25 g/l NaCN, 1 g/l ZnO and 0.03 g/l  $\text{Ni}(\text{CH}_3\text{COO})_2$  respectively. These solutions are used as electroplating baths for producing CMM coatings which are done under current densities of 20 and  $10 \text{ mA/cm}^2$  respectively for depositing thin layer of Yellow and White Miralloys. Depending on the thickness of individual thin layer, each electroplating process is carried out with different electroplating time and it is estimated from the results of earlier experiment. CMM coatings with different thin layer thickness (from 1000 nm down to 20 nm) are proposed to be deposited on mild steel substrates. The relationships between the maximum individual layer thickness and its mechanical properties (e.g. micro hardness) as well as the thickness of individual layer at which the superior properties of CMM begin to appear will be determined.

#### **1.4 Expected Outcomes**

The expected outcomes of these experimental works are the electroplating conditions that are appropriate for producing binary and quaternary Yellow and White Miralloys. These will be further implemented for automotive and probably also for the electronic applications. Experimental results are also expected to give additional information in the kinetics of codeposition of Cu-Sn and the influence of electroplating bath composition and current density on the coating composition, phases present within the coating, microhardness and corrosion resistance of the coatings. The possibility to increase microhardness of coating by producing such the CMM coating has been expected as the main outcomes of the current experimental works.

## **CHAPTER 2**

### **LITERATURE REVIEW**

#### **2.1 Electroplating**

Metal finishing is the name given to a wide range of process carried out in order to modify the surface properties of a metal, e.g. by the deposition of a layer of another metal alloy, composite, or by formation of an oxide film. The origins of the industry lay in the desire to enhance the value of metal articles by improving their appearance, but in modern times the importance of metal finishing for purely decorative reason has decreased. The trend is now towards surface treatment which will impart corrosion resistance or particular physical or mechanical properties to the surface (e.g. electrical conductivity, heat or wear resistance, lubrication or solderability) and hence, to make possible the use of cheaper substrate metals or plastics covered to give them essential metallic surface properties. It should be emphasized that not all surface finishing is carried out using electrochemical methods, but electroplating is still represents a large portion of the metal finishing industry.

The objective of an electroplating process is to prepare a uniform deposit which adheres well to the substrates and which has the required mechanical, chemical and physical properties. Moreover, it is of overriding importance that the deposit properties meet their specification on all occasions, i.e. the process is both predictable and reproducible. On the other hand, many metals may (by modification of the bath and electroplating conditions) be deposited with different properties. It is for this reason that it is not possible to define a single set of conditions for electroplating of each metal; the bath, current density, temperature, etc., these will depend to some extent on the deposit properties required.

It is important that the plating bath is stable for a long period of time because of the importance of the reproducibility of the deposit. It is also necessary that the quality of deposit is maintained over a range of operating conditions, since some variations in concentrations and current density are bound to occur, particularly when different objects are to be plated. Tolerance of the bath to carry over from previous process liquors or mishandling during operation on the factory floor is an additional advantage.

The principle components of an electroplating process are shown schematically in Figure 2.1. The essential components include:

1. An electroplating bath containing a conducting salt and the metal to be plated in a soluble form, as well as perhaps a buffer and additives.
2. The electronically conducting cathode, i.e. the workpiece to be plated.
3. The anode (also electronically conducting) which may be soluble or insoluble.
4. An inert vessel to contain (1)-(3), typical, e.g. steel, rubber-lined steel, polypropylene or polyvinylchloride.
5. A direct current source, usually a regulated transformer/rectifier.

Metal electroplating is the process of electrolytically depositing layer of metal, alloy or metal matrix composite onto a surface. The object to be plated is made as a cathode/cathodes in an electrolyte bath containing a simple cation (e.g.  $M^{n+}$ ) or a complex metal ions (e.g.  $M(CN)_2^-$ ). So that the example of possible reactions that can occur at the cathode during a single metal electroplating are:



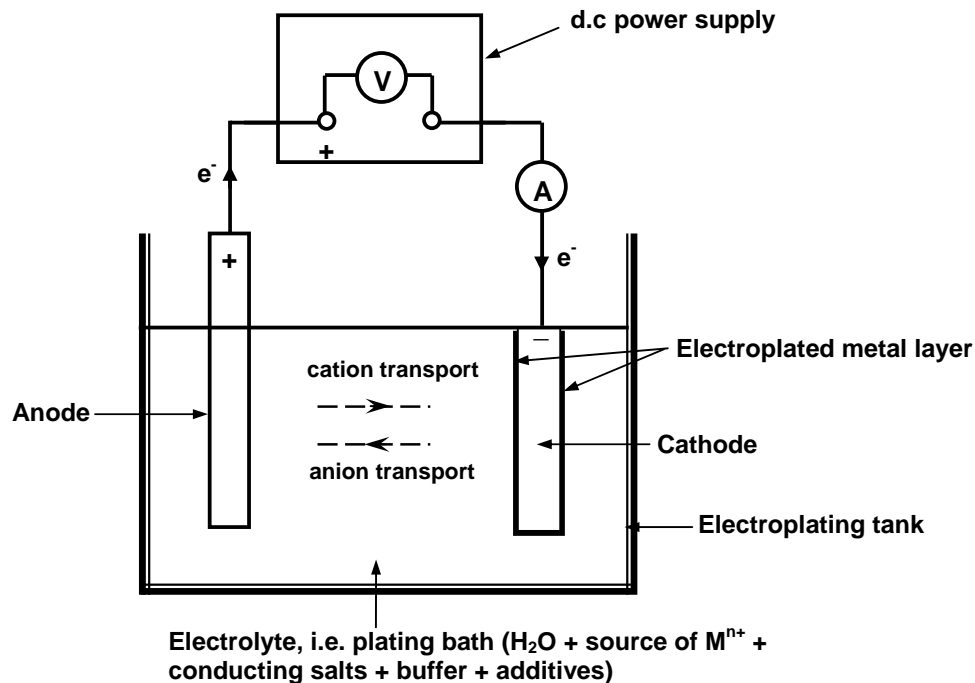
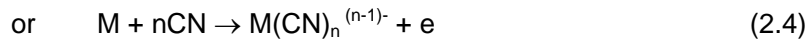


Figure 2.1: Component of Electroplating

Hence, the metal ion may be a simple ion such as hydrated  $\text{Cu}^{2+}$  or it may represent a metal complex such as  $[\text{Cu}(\text{CN})_2]^-$ . Where possible, the preferred anode reaction is the dissolution of the same metal to its precursor in solution.



In ideal, the electrolysis conditions are controlled in such a way that the current efficiencies of reaction (2.1 or 2.2) and (2.3 or 2.4) are the same and, hence, the concentration of  $\text{M}^{n+}$  or metal complex ion in the bath remains constant. In a few cases, the metal ion has to be added as a solid oxide and then an inert anode is employed; the main anode reaction is oxygen evolution. For a successful electroplating process, the correct pretreatment of the cathode and careful selection of the anode material, plating bath, current density and other electrolysis condition, are essential. By using proper type of electroplating baths and adjusting its composition as well as

electroplating parameters such as current density and temperature, following type of layer may be electroplated:

1. Single metals: the most important are Sn, Cu, Ni, Cr, Zn, Cd, Pb, Ag, Au and Pt.
2. Alloys including: Cu-Zn, Cu-Sn, Pb-Sn, Sn-Ni, Ni-Co, Ni-Cr, Ni-Fe, Cu-Sn-Zn, and Cu-Sn-Zn-Ni.
3. Composites: i.e metals containing dispersed solid such as PTFE, Al<sub>2</sub>O<sub>3</sub>, WC, diamond, SiC, Cr<sub>3</sub>C<sub>2</sub> and graphite.
4. Multilayers: including multiple alternate layer of Cu and Ni; Ni and Fe; Cu and Co; Cu and Ag; Fe and Pt; Zn and Zn-Ni; Ni-P and Ni etc.

The mass of metal  $w$  (g) deposited during electroplating may be expressed in terms of Faraday's laws of electrolysis as follows

$$w = \frac{\phi \tilde{M} q}{n F} \quad (2.5)$$

where  $\tilde{M}$  is the mol weight of metal (g/mol),  $q$  is equal to  $It$  (A.sec.) namely as the electrical charge,  $n$  is the moles of electron that gets involve in the half cell reaction per 1 mol metal deposited and  $\phi$  ( $\leq 1$ ) is the cathode current efficiency for metal deposition. The majority of electroplating processes are carried out batchwise, at a constant current density  $I$  for a measured time  $t$ . The averaged rate of mass deposition per unit area is then given by:

$$\frac{w}{A t} = \frac{\phi I \tilde{M}}{A n F} \quad (2.6)$$

where the factor  $\tilde{M} / n F$  is the electrochemical equivalent (g/A.sec.) and  $A$  is the surface area (cm<sup>2</sup> or m<sup>2</sup>). This expression can also be written in terms of the useful current density ( $i$ ).

$$\frac{w}{A t} = \frac{\phi i \tilde{M}}{n F} \quad (2.7)$$



Thus the rate of deposition depends upon the current density, the molar mass of the metal  $M$ , the number of electrons  $n$  per mole of  $M^{n+}$  and the prevailing current efficiency  $\phi$ .

## **2.2 Thermodynamic of Electrodeposition**

Information contained in potential-pH diagrams is useful in several ways for application to problems involved in electroplating, for cathodic and anodic processes as well as the stability of solution.

### **2.2.1 Cathodic Processes**

The desired cathodic reaction in electroplating is ordinarily metal deposition. In most electroplating processes, dissolved oxygen reduction also occurs at the cathode, while hydrogen ion reduction is undesirable and may cause coating embrittlement and produce an uneven coating surface. As an example, consider potential-pH equilibrium diagram for Ni-H<sub>2</sub>O system at 25°C (Figure 2.2). Nickel can be deposited from acid and alkaline solutions. It is obvious, most of nickel electroplating is done from nickel sulphate solutions open to air because the stability of nickel sulphate solution appears in a wide range of pH. At, say, pH 4.5 and potential ( $E$ ) = -0.4 Volt, evidently dissolved oxygen and hydrogen ions can be reduced as well as nickelous ions; however, the overpotentials required to reduce dissolved oxygen and hydrogen ion at sensible rates are fortunately considerably higher than that required for nickelous ion reduction, and this can consequently result in efficiency less than 100 % (e.g. 96 %). Decrease of pH tends to increase the relative amount of hydrogen ion reduction. Nevertheless, the acid type of Watts nickel bath operating at pH 2 can give good nickel deposition even though, somewhat more hydrogen is evolved, because the pH of the solution at the cathode interface rises, through hydrogen ion reduction and under steady-state deposition conditions the relative amount of hydrogen ion reduction is not unduly large.

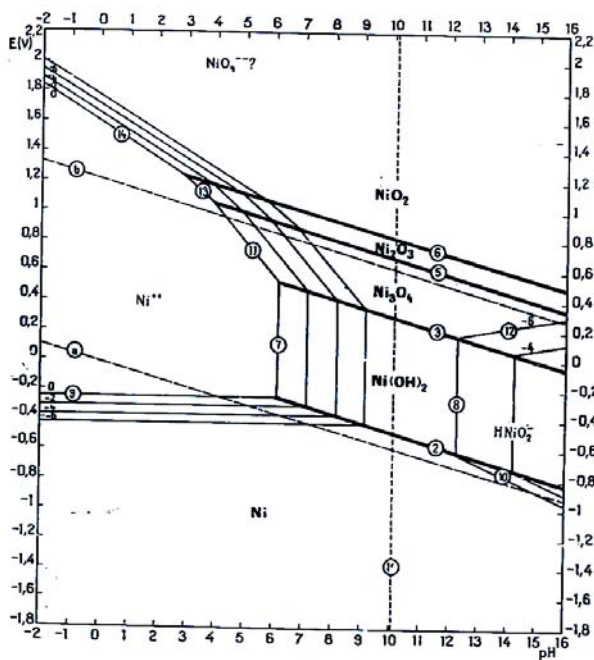


Figure 2.2: Potential-pH diagrams for Ni-H<sub>2</sub>O system at 25 °C [Pourbaix, 1974]

On the other hand, increase of pH of the bulk solution beyond about 5 causes the catholyte under deposition conditions, to contain sufficient nickelous hydroxide (Ni(OH)<sub>2</sub>), present as positively charged colloidal particles, to lead to co-deposition of hydroxide with metal; this gives a harder and more brittle deposit that, although suitable for rather limited purposes, is in general undesirable. The very small Faradic current required for hydroxide or oxide deposition, due to the small charge/mass ratio of the colloidal particles, explains why a high pH nickel bath may give almost 100 % cathode current efficiency and yet yield deposits containing considerable hydroxide.

### 2.2.2 Anodic Processes

In electrodeposition, it is usually desired to have either (a) an anode of the metal being deposits that dissolved at near 100 % current efficiency or (b) an anode that is totally insoluble and that acts merely as an inert basis for oxygen evolution. It is rarely

desirable to have an anode that gives mixture of these processes, or that operates consecutively in the dissolving and the passive state.

For example, nickel dissolves to nickelous ions at unit activity, at potentials more positive than  $-0.23$  V and at pH less than about 6. At higher pH, solid nickelous hydroxide is the initial anodic product, and this is converted to higher oxides at higher anode potentials, under such conditions, passivation of a nickel anode occurs at once. However, passivation can also occur below pH 6, indeed, as low as pH 0.5 because the anodic overpotential required to dissolve nickel to nickelous ions at the current densities required in electrodeposition process is considerable. Thus, if the polarization raises the anode potential above the broken line extension of the  $\text{Ni}/\text{Ni}(\text{OH})_2$  line (Figure 2.2), solid nickelous hydroxide may be formed at low pH, and since there is good evidence that its formation from the metal is kinetically easier than the formation of dissolved nickelous ion, its preferential formation is not surprising, and the tendency of nickel anodes to passivate is easily understood. In practice, this is remedied by the incorporation of a little oxide in the nickel anode and/or of chloride in the solution; the overpotential required for dissolution is thereby much reduced and the potential for passivation is not reached.

Soluble anode operating in alkaline solution, such as tin and zinc, can also passivate at high current densities, mainly because the supply of complexing hydroxyl ions in the solution next to the anode become insufficient, so that insoluble hydroxides or oxides are formed. In the special case of tin anodes required to dissolve as stannate rather than stannite, a pseudo-passivation effect of this kind is advantageous; the anode is first passivated by the formation of stannic oxide at high current density, and subsequent operation at lower current density enables the stannic oxide to dissolve in the alkaline solution as stannate while being reformed anodically at the same rate. The

potential-pH conditions for these transformations can be seen in the diagram for tin (Figure 2.3).

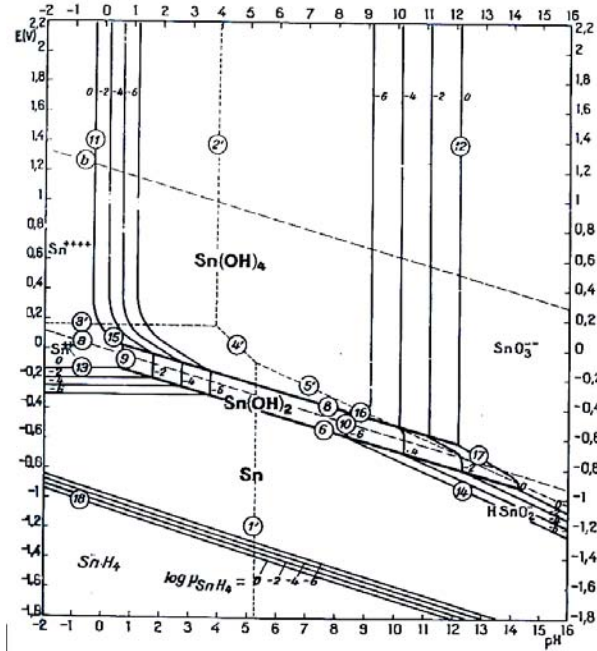


Figure 2.3: Potential–pH diagrams for Sn–H<sub>2</sub>O system at 25 °C [Pourbaix, 1974]

## 2.3 Kinetic and Mechanism of Electrodeposition Process

### 2.3.1 Relationship between Current and Potential

In electrodeposition, the basic parameter which causes deposition to occur is the potential at cathode. For any electrodeposition to take place, a current has to flow through an electrochemical cell. When a net current flows through an electrochemical cell, the electrode potential deviates from its equilibrium value. The difference between the actual electrode potential ( $E_a$ ) and the equilibrium potential ( $E_e$ ) is the overpotential ( $\eta$ ). It can be expressed by

$$E_a = E_e + \eta \quad (2.8)$$

Activation overpotential refers to the energy needed to move ions across the interface between electrolyte and electrode and to build the discharged atom (adatom) into the

crystal structure of the cathode deposit. For a single step process the current in an activation controlled process responds to the electrode potential according to the Butler-Volmer equation [Bockris and Reddy, 1977]:

$$i = i_o \left[ \exp \left( \frac{\beta n F}{R T} \eta \right) - \exp \left( - \frac{(1-\beta) n F}{R T} \eta \right) \right] \quad (2.9)$$

where  $i_o = n F k_o C \exp \left( \frac{\beta n F}{R T} E_e \right)$

In the above equations,  $k_o$  is a rate constant;  $i_o$  is the exchange current density;  $C$  is the concentration of the metal ions at the interface and  $E_e$  is the equilibrium potential of the electrode.  $\beta$  is the symmetry factor defined in terms of the ratio between distance across double layer to summit of activation energy and distance across whole double layer. To describe a multi-step process,  $\beta$  must be replaced by an experimental parameter,  $\alpha$ , which is called the transfer coefficient. Equation (2.9) retains a form which emphasizes that the measured current density at certain overpotential is the sum of the partial cathodic and anodic current densities. When  $\eta$  is very low, say,  $\eta < 10$  mV and  $\bar{\alpha} = \bar{\alpha} = 0.5$ , a limiting form of current density can be obtained

$$i = i_o (F / R T) \eta \quad (2.10)$$

Equation (2.10) shows that  $i$  depends linearly on  $\eta$ . Another limiting form is when  $\eta < -52$  mV and the first term in the Butler-Volmer equation becomes negligible compared with the second. The equation applying to this region can be written as:

$$\log |-i| = \log i_o - \frac{\bar{\alpha} F}{2.303 R T} \eta \quad (2.11)$$

which is known as the cathodic Tafel equation. Similarly, positive overpotentials greater than 52 mV lead to the anodic Tafel equation. Figure 2.4 shows a  $\log |i|$  vs  $\eta$  curve for a solution and the exchange current density and transfer coefficients are obtained from the intercepts and slopes.

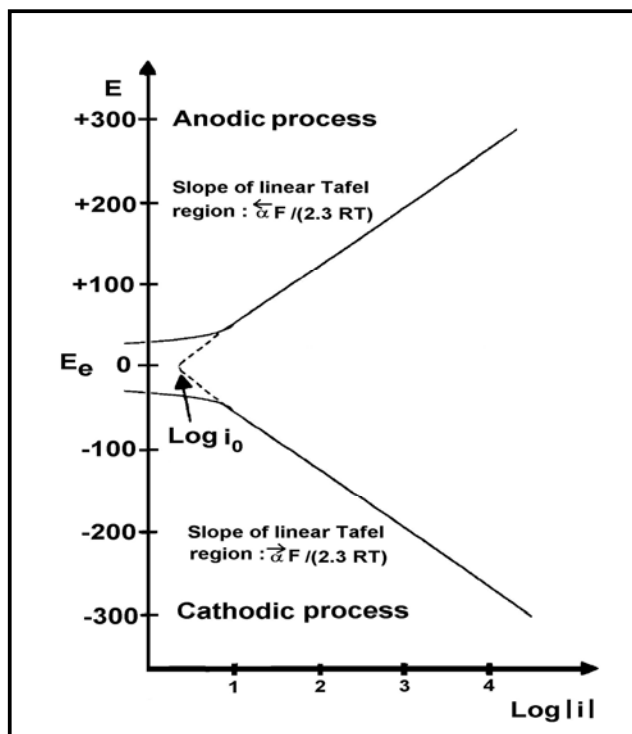


Figure 2.4: Plot of  $\log |i|$  vs  $\eta$

### 2.3.2 Influence of Mass Transport on Electrode Kinetics

The current-potential relationship defined by equation (2.9), (2.10), and (2.11) is valid for the case where electrode process is being controlled by the charges transfer. Under the condition of mass transport control, the electrode reaction rate is determined by the diffusion rate of the electroactive species. The concentration of the electroactive species at the interface between electrode and electrolyte is lower than that in the bulk solution. The concentration overpotential is expressed as follows:

$$\eta_c = 2.303(RT/nF) \log(1 - i/i_L) \quad (2.12)$$

where  $i_L$  is the limiting current density, which is defined as a current density at the maximum rate of mass transport of electroactive species through the diffusion layer. This occurs when the concentration of electroactive species at interface approaches zero. By referring to first Fick's equation, the limiting current  $i_L$  that is independent of potential might be written as

$$i_L = \frac{n F D C_0}{(1 - t_+) \delta} \quad (2.13)$$

where  $D$  is the diffusion coefficient,  $C_0$  is the bulk concentration, and  $\delta$  is the diffusion layer thickness and depends on the diffusion,  $t_+$  is the transfer number of electroactive specie and convection conditions in the bath. The essence of mass transport is the quantity  $\delta$ . Decreasing  $\delta$  can increase  $i_L$ . Stirring the solution will decrease the effective value of  $\delta$ . When the process is a mixed control, the activation and mass-transport processes always occur in series and they combine to determine the overall rate. A general qualitative description of the relationship between current density and potential is shown in Figure 2.5 [Gileadi, 1993].  $i_L$  is the limiting current density controlled by mass transport.

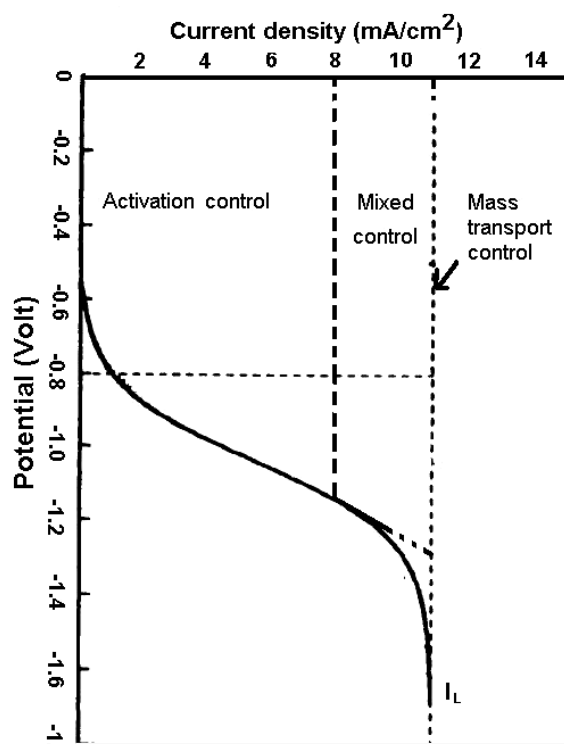


Figure 2.5: A general qualitative description of the relationship between current density and potential [Gileadi, 1993]

Diffusion layers are not formed immediately upon the application of potential, but require several seconds or perhaps a minute, to be formed, depending on the rate of agitation. On flat electrodes, thickness increase infinitely with time if there is no convection. At the flat vertical electrodes,  $\delta$  is fairly constant over most of the surface, unless there are local variations in the rate of agitation but it is much smaller near the leading edge, where the streaming electrolyte first encounters the electrode, and especially on corners [Gileadi, 1993].

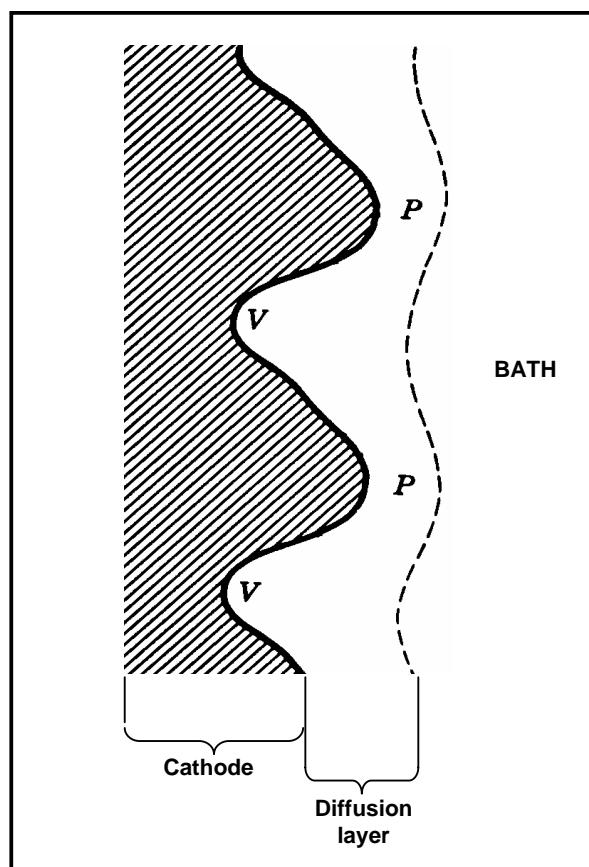


Figure 2.6: Schematic cross-section showing microroughness of cathode, at peaks (P), supply of electroactive species is relatively rapid over the short distance from the diffusion boundary, whereas at valley (V) it is too slow [Paunovic and Schlesinger, 1998].



The cathode surface is never entirely smooth. If the roughness profile has dimensions about equal to the thickness of the diffusion layer, or somewhat smaller, its thickness varies between micropeaks and microvalleys; it cannot follow the contours, but is smaller over the peaks (Figure 2.6). During deposition, local thickness differences in the diffusion layer affect a different supply of electroactive species toward the cathode. On peaks diffusion layer is thin, and supply of ions faster than in microvalley where there is a thicker diffusion layer.

### **2.3.3 Hydrogen Evolution**

The above elementary discussion of deposition reaction was aimed at giving the first essentials of how metal is deposited. However, the simultaneous reduction reaction of two or more electroactive species may occur during electroplating. This arises from the fact that one sometimes finds that there is less metal deposited than there should be on the basis of Faraday's laws, which requires that the deposition of one gram equivalent of metal per faraday of electricity passed through the system. In fact, in some cases, there is almost no deposit at all. In such cases, hydrogen evolution is occurring. From a technological point of view, however, one seeks to deposit a metal without wastage of electrical energy on hydrogen evolution. Basically, increases current density higher than the limiting current density for the deposition of the metal is due to hydrogen evolution. In aqueous solutions hydrogen will always be evolved if the total deposition current is made sufficiently high; the hydrogen may come not only from  $H^+$  (of limited concentration) but also from the water itself. The effects of hydrogen co-deposition on the crystallography of metal deposition are widespread and rather complicated. Several starting paths to new effects and mechanisms may be noted, however. Hydrogen atoms may adsorb more freely on certain crystal planes and block them so that the metal grows preferentially on others. The development of a preferred orientation of the deposit crystals can sometimes be ascribed to the preferential adsorption of hydrogen on certain crystal facets (Bockris and Reddy, 1977). Hydrogen

may also permeate into the metal and change its mechanical properties. Finally, removal of  $H^+$  ions from the diffusion layer near the electrode changes its properties, too, it makes the solution at interface becomes more alkaline. If the hydrogen reaction leads to produce a sufficiently alkaline solution at interface, the solubility product of a hydroxide of the metal ion present will be exceeded, which would cause precipitation and may be contaminated the coating. Thus, hydrogen co-deposition produces many things and they are usually destructive. The hydrogen evolution reaction from aqueous solution can be presented as,

in acid solutions, the overall reaction is



and in alkaline solutions, it is only



It should be noted however, in several electroplating cases such as zinc electroplating in acid bath, hydrogen evolution reaction cannot be avoided.

#### **2.3.4 Atomic Aspects of Electrodeposition**

Electrodeposition or electrocrystallization is the process in electroplating where the incoming metal ions are reduced and then join the metal deposit. The rate of incoming metal ions is the main factor related to the structure formed. A low rate (low current, low polarization) favors the growth of existing nuclei, while a high rate (high current, high polarization) favors the formation of new nuclei. Other factors, which affect the structure of the deposit, are the surface finish of the base metal, and the effects of solution additive which are adsorbed onto the cathode surface and inhibit the growth pattern [Doesburg and Ivey, 2000].

Electrocrystallization has two competing processes: nucleation and grain growth. If a deposition starts on an electrode surface of a different material, that of the

object to be plated, the first step will be the formation of nuclei of the new phase and their growth into crystals with the characteristic lattice. Then, once the electrode surface is fully covered by a few atomic layers of this metal, the layer is thickened into a macroscopic deposit. Nucleation is an improbable event and is achieved at an electrode surface by the application of a large overpotential. The nuclei, once formed, grow quite rapidly at comparatively low overpotentials, and in constant-current operation. The overpotential will decrease substantially once nucleation has occurred. The growth of the crystals occurs by incorporation of the individual metal atoms into the crystal lattice [Sun, 1998].

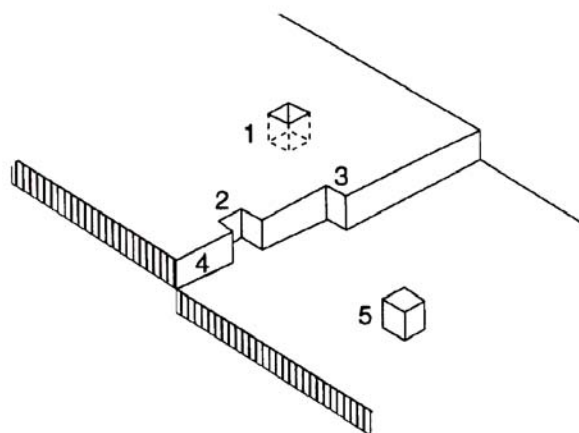


Figure 2.7: Discharge site on a growing surface: (1) surface vacancy; (2) ledge vacancy; (3) ledge kink; (4) ledge; (5) layer nucleus [Gabe, 1978; Pletcher and Walsh, 1990; Paunovic and Schlesinger, 1998; Doesburg and Ivey, 2000]

In general, electrocrystallization is the incorporation of the metal atoms into the crystal lattice of the cathode during electroplating. There are two main factors, which determine the type of structure, which is formed. The first is the current density, which is directly related to the rate of incoming atoms, and the second is the inhibition of the cathode surface by adsorbed substances. There are various sites on the cathode surface onto which an atom can become attached. The different types of sites are identified in Figure 2.7 [Gabe, 1978; Pletcher and Walsh, 1990; Paunovic and Schlesinger, 1998; Doesburg and Ivey, 2000]. A surface vacancy (1) has minimum

energy, but these types of sites are not present in large numbers. Ledge sites (2, 3 and 4) are favorable for growth because they are repeatable steps. Once an adatom (one neighbor) or adion diffuses to a ledge or ledge kink (where the atom can interact with three neighbors) and is incorporated into the lattice, the same ledge structure is present for the next growth step. The nucleation of a new layer (5) requires the most energy.

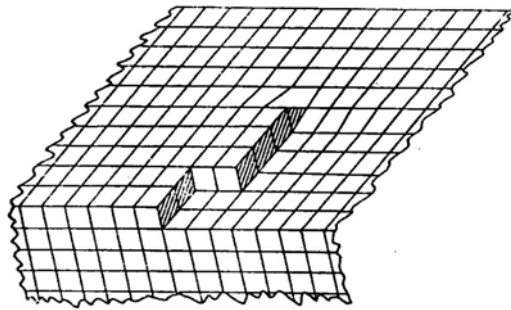


Figure 2.8: Growth screw dislocation with a kinked growth ledge

A screw dislocation mechanism of crystal growth was proposed by Doesburg et al. [2000], and allows growth without the need for nucleation of new layers. In this manner a screw dislocation with the Burgers vector perpendicular to the crystal face grows by the ledge mechanism, winding itself up like a spiral staircase (Figure 2.8) [Gabe, 1978]. The screw dislocation mechanism is a rare case in electroplating and operates at low current densities and overpotentials, where there is enough time for the adions or adatoms to diffuse to the growth ledge and the overpotential does not support the formation of new nuclei. This type of growth has been observed for copper plated at low current densities from very pure sulfate solutions [Gabe, 1978; Pletcher and Walsh, 1990; Paunovic and Schlesinger, 1998].

### 2.3.5 Growth Mechanism

According to Paunovic and Schlesinger [1998], there are two basic mechanisms for formation of coherent deposit: layer growth and three-dimensional (3D) crystallites growth (or nucleation-coalescence growth). A schematic illustration of these two mechanisms is given in Figure 2.9. In the layer growth mechanism a crystal enlarge by a spreading of discrete layer (steps), one after another across the surface. In this case a growth layer, a step, is a structure component of a coherent deposit. Steps, or growth layer, are the structural deposition of metals (e.g., columnar crystal, whiskers, and fiber texture). It can be distinguished among monoatomic steps, polyatomic microsteps, and polyatomic macrosteps. In general, there is a tendency for a large number of thin steps to bunch into a system of a few thick steps. Many monoatomic steps can unite (bunch, coalesce) to form a polyatomic step.

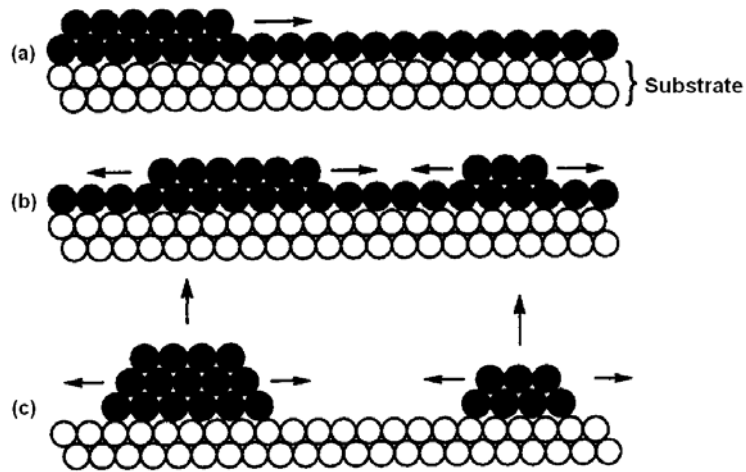


Figure 2.9: Schematic representation of layer growth (a,b) and the nucleation-coalescence mechanism (c) [Paunovic and Schlesinger, 1998]

In the 3D crystallites growth mechanism the structural components are 3D crystallites and a coherent deposit is built up as a result of coalescence (joining) of these crystallites. The growth sequence of electrodeposition via nucleation-coalescence consist of four stages: (1) formation of isolated nuclei and their growth to

TDC (3D crystallites), (2) coalescence of TDC, (3) formation of linked network, and (4) formation of a continuous deposit.

The structure of the growing layer is determined largely by the relative rates of electron transfer to form an adatom and diffusion of the adatom across the surface into a position in the lattice, and the electrolysis conditions, including bath additives which may radically modify the electrocrystallization process. At low current density, the surface diffusion is fast compared with electron transfer and the adatom is likely to end up in a favored site in the lattice. At higher current densities, surface diffusion is no longer fast compared with electron transfer and further nuclei must form; the layer will be less ordered [Gabe, 1978; Pletcher and Walsh, 1990]

During the thickening stage a key parameter is the current density. At low current densities, surface diffusion is fast compared with electron transfer and both the crystal lattice and structures such as screw dislocations can be well formed. The predominant orientations of surface planes can also be determined using electron diffraction. At high current densities, adatoms no longer reach their equilibrium position in the lattice and nucleation of additional growth centers remains a more frequent event. Hence the lattice formed will be less ordered and macroscale features, such as steps, ridges and polycrystalline block growth become more likely. With further increase in current density, outward growth of the layer becomes of increasing importance and problems arising from mass transport control in solution can arise, e.g. dendrites. Once this form of growth commences, it predominates because of the enhanced rate of mass transport to the tip and the  $iR$  drop to the tip is also a minimum as this is the closest point to the anode. A powdered texture usually results in the completely mass-transport-controlled potential region.

Crystal growth mode is a strong function of overpotential and current density, as shown in Figure 2.10. Displacement from the equilibrium potential not only results in increasing current, but also influences the morphology of the deposit. At low overpotentials, current density is low and crystal growth is epitaxial. Epitaxial growth occurs when the lattice structure of the deposit is oriented the same direction as crystals in the substrate.

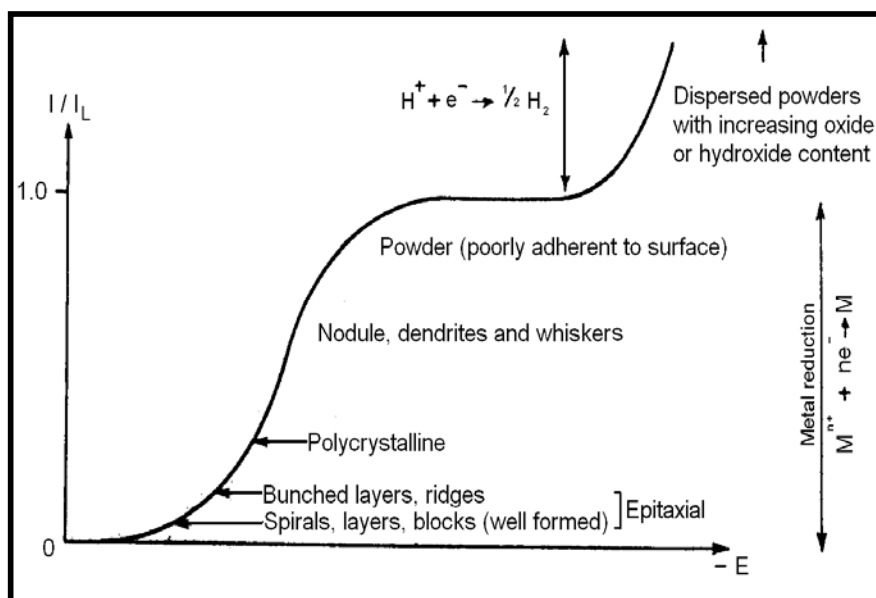


Figure 2.10: Dependence of crystal growth mode and current density on overpotential [Gabe, 1978; Pletcher and Walsh, 1990]

As overpotential increases, the nature of the deposit changes until the limiting current is reached and the deposit is powdery. At even higher overpotentials hydrogen evolution ensues, the pH at the electrode surface becomes increasingly basic, and oxides or hydroxides may be incorporated into deposit. Since epitaxial deposits exhibit superior adhesive qualities [Dini, 1993], strike-plating baths are often operated at low overpotentials and current densities. Cyanide copper strike baths typically operate at 10-30 mA/cm<sup>2</sup>, and copper pyrophosphate baths typically operate at 10-75 mA/cm<sup>2</sup> [Durney, 1984]. For purposes of comparison, copper sulfate plating baths operate at 30-500 mA/cm<sup>2</sup> [Lowenheim, 1978].

Carneval and Cusminsky [1981] reinvestigated the influence of current density on the morphology of copper deposits from cyanide, pyrophosphate, sulfate, chloride, and citrate electrolytes. They determine the deposit thickness at which the morphology of the deposit changed from epitaxial to polycrystalline, and observed that as current density increased, the thickness at which the deposit morphology changed to polycrystalline decreased. For cyanide deposits, the transition occurred at 8-10  $\mu\text{m}$  for current densities in the 10-30  $\text{mA}/\text{cm}^2$  range. They found that the thickness which the deposit changes to polycrystalline was highest for the smallest anion,  $\text{Cl}^-$ , and least for the largest anion,  $\text{P}_2\text{O}_7^{4-}$ . The effect that the anion has on the morphology of the deposit was greater at higher current densities than it was at lower current densities.

### 2.3.6 Development of Columnar Microstructure

The columnar microstructure is perpendicular to the substrate surface, is shown schematically in Figure 2.11. This microstructure is composed of relatively fine grains near the substrate but then changes to a columnar microstructure with much coarser grains at greater distances from the substrate.

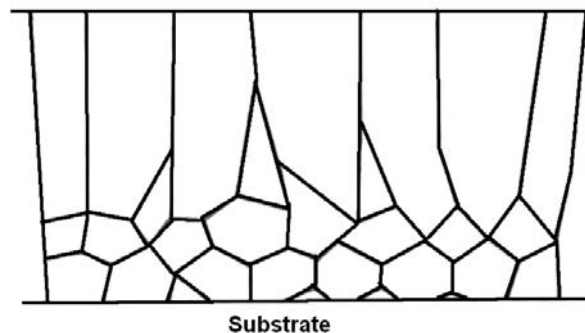


Figure 2.11: Schematic cross section (perpendicular to the substrate) of the columnar deposit [Paunovic and Schlesinger, 1998]



The development of the columnar microstructure may be interpreted as the result of growth competition among adjacent grains. The low-surface-energy grains grow faster than the high-energy ones. This rapid growth of the low-surface-energy grains at the expense of the high-energy grains results in an increase in mean grain size with increased thickness of deposit and the transition from a fine grain size near the substrate to a coarse, columnar grain size [Paunovic and Schlesinger, 1998].

## **2.4 Electrodeposition of Alloy**

A large proportion of cast or wrought metals are alloys rather than pure metals. This is because the properties of alloys vary over a wider range than those of pure metals, and thus alloys can be designed to meet most of the mechanical or chemical requirements more satisfactorily than pure metals. On the other hand, electrodeposits are mostly unalloyed and are usually produced and used in a state of fairly high purity. In fact, a lot of efforts are made to keep the plating baths free of metallic contamination. This is not because the electrodeposited alloys are not desirable, but because (1) the closer control required for the alloy deposition complicates commercial electroplating processes, (2) the properties of the electrodeposited alloys are not adequately known. Another less important reason is that, electrodeposited metals, even at high purity, can display broader properties according to the service requirement, by controlling the plating process [Kanani, 2004].

The most important practical consideration involved in the co-deposition of two metals is that their deposition potentials should be fairly close together. The importance of this consideration follows from the well-known fact that the more noble metal deposits preferentially, frequently to the extent that the less noble metal can not be deposited at all. Therefore, to simultaneously co-deposit the two metals, conditions must be such that the deposition potential of the less noble metal can be attained without employing an excessive current density. Hence, it is necessary to have the

potentials of the two metals close together [Gabe, 1978; Paunovic and Schlesinger 1998].

The table of standard electrode potentials, Table 2.1 may serve as a rough guide for deciding if two metals may be co-deposition from a simple salt solution [Gabe, 1978]. The electrode potentials in Table 2.1 apply only to the equilibrium potentials of the metals in a solution of their simplest ions with unit concentrations. These potentials are just theoretically the most positive (most noble) potentials at which the metals can be deposited. In actual deposition, because of polarization, the deposition potentials are more negative than the equilibrium potentials.

Table 2.1: Standard reduction electrode potentials at 25 °C [Gabe, 1978]

Metal couple	E° (Volts)
Au <sup>3+</sup> /Au	+ 1.50
Au <sup>+</sup> /Au	+ 1.70
Ag <sup>+</sup> /Ag	+ 0.799
Cu <sup>+</sup> /Cu	+ 0.52
Cu <sup>2+</sup> /Cu	+ 0.337
Bi <sup>3+</sup> /Bi	+ 0.317
Cu <sup>2+</sup> /Cu <sup>+</sup>	+ 0.153
Sn <sup>4+</sup> /Sn <sup>2+</sup>	+ 0.15
Al <sup>3+</sup> /Al	- 1.66
Zn <sup>2+</sup> /Zn	- 0.763
Fe <sup>2+</sup> /Fe	- 0.44
Co <sup>2+</sup> /Co	- 0.277
Ni <sup>2+</sup> /Ni	- 0.25
Sn <sup>2+</sup> /Sn	- 0.136
Pb <sup>2+</sup> /Pb	- 0.126

Approximately, the potentials of Table 2.1 represent the potentials of metals in slightly acid solutions of the simple salts, such as the chloride or sulfate. In solutions of metals complex ions their potentials are more negative (less noble) than in their uncomplexed states. Therefore this table can be utilized to derive some conclusions regarding alloy deposition from acid solutions of simple ions. Metals which are close together in Table 2.1 should generally be more readily co-deposited than metals which are widely separated. For example, lead and tin, nickel and tin, copper and bismuth,

nickel and cobalt can be readily co-deposited to form alloys, because their potentials are less than 0.1 volt apart. On the other hand, silver and zinc do not co-deposit readily because of their potential difference of 1.5 volts apart.

For metals with rather large differences potentials as listed in Table 2.1, their potential can be brought closer together by (a) increasing the current density, (b) adjusting the concentration of species in solution, which can be achieved by introducing complexants and (c) using organic additives to preferentially inhibit the deposition of the more noble metal. However, these factors are effective only if the polarization of the more noble metal is increased to a larger extent than is that of the less noble metal [Zhang and Abys, 2000]. Brenner has listed five types of deposition system:

- (1) Regular solutions under diffusion control. Uncomplexed metal ions and two metals of widely differing nobility.
- (2) Irregular solution under cathode potential control. Static potential affected by complexing alone; e.g. cyanide bath for copper-zinc alloys.
- (3) Equilibrium solutions where at low current densities the bath metal concentrations give the deposit metal directly; e.g. lead-tin alloys from acid baths.
- (4) Anomalous solutions in which the less noble metal deposits preferentially; e.g. iron, cobalt or nickel.
- (5) Induced solutions in which a metal can be co-deposited as an alloy although it will not deposit singly; e.g. molybdenum or tungsten with iron group metals.

The first three are classed as normal systems in that the proportions of metal deposited may be estimated on the basis of the polarization curves of the individual metals. If the two metals have similar polarization curves (Figure 2.12(a)) the deposit weight ratio is  $i_1 z_1 / i_2 z_2$  where  $i_1$  and  $i_2$  are the individual current densities and  $z_1$  and  $z_2$  are the

respective electro-chemical equivalents. If the degrees of polarization are different (Figure 2.12(b)) the deposit composition depends upon the potential.

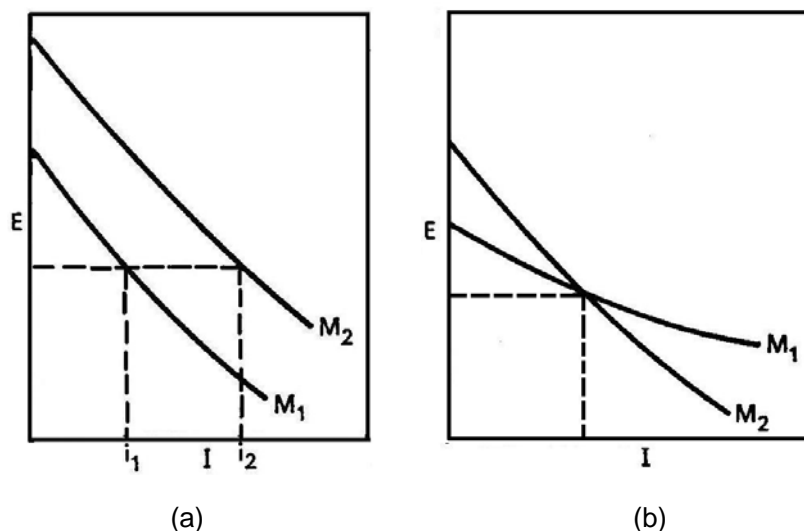


Figure 2.12: Polarization behavior for co-deposition of metals M<sub>1</sub> and M<sub>2</sub>. (a) M<sub>1</sub> and M<sub>2</sub> having similar E/i curves, (b) M<sub>2</sub> polarizing more than M<sub>1</sub> [Gabe, 1978]

At the point intersection  $i_1 = i_2$  and the weight ratio in the deposit must be  $z_1 / z_2$ , but below this potential (more positive) the ratio is less while at more negative potential the ratio is greater. The overall deposition rate ( $i_1 z_1 + i_2 z_2$ ) also varies with potential, of course. In general alloy electrodeposits give corrosion resistances superior to those of their constituents. This is particularly true for tin-nickel alloys, which are stable in cold nitric acid and are not tarnished by foodstuffs of a sulphur-staining kind. At present applications are relatively specialized, but the copper alloys have found wide application for decorative use in the cosmetic jewellery field where their tarnish resistance make their substitution for gold realistic. Other alloys having specific application include cadmium-zinc for protection, iron-zinc for decoration and protection and nickel-iron for magnetic shielding.

### 2.4.1 Structure of Electrodeposited Metal / Alloys

In the majority of electrodeposited materials, the atoms are arranged in a uniform, three-dimensional array. The volume over which this arrangement extends uniformly is called, when many crystals form a solid material, they are called grains. If the array of atoms is random, the material is amorphous. However, in materials considered to be amorphous, there are generally still very small groups of atoms that possess the same arrangement as crystals.

Most electrodeposits exist in one of three crystal habits (Figure 2.13). The most common one is face-centered cubic (fcc) in which atoms or atom groups are located at the corners of a cube and in the center of its faces. Another common crystal structure is body-centered cubic (bcc) in which atoms or atom groups are located at the corners of a cube and in its center. Materials less often have the hexagonal structure. The atomic arrangement of the basal plane of the cube diagonal of the face-centered-cubic one. The habits only differ in the third atom layer.

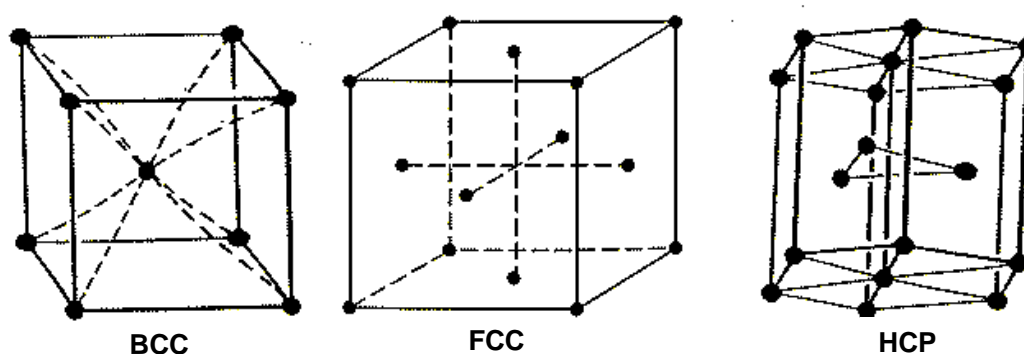


Figure 2.13: Unit cells of the three most importance lattices

In many electrodeposits there is a crystal direction that grows faster toward the anode than the other ones. Grains possessing this direction can also grow sideways and cover the less favorably oriented ones. They can grow sideways until they encounter grains of the grains possessing the favorable growth direction. If the grains are not

randomly oriented, the condition is called a texture. In the case of electrodeposits the texture is a fiber axis because just as in a wire drawn through a die, the directions perpendicular to preferred orientation are randomly oriented. When electrodeposits are annealed, they generally recrystallize, the texture often changes.

## 2.4.2 Properties of Electrodeposited Metal / Alloys

The properties of metallurgical metals and alloys (cast or wrought) have been studied comprehensively, and this knowledge has led to extensive and varied uses. With the growth of technology, electrodeposits are also more and more applied to a variety of engineering and scientific purposes and, consequently, more interest is shown in their properties.

Table 2.2: Vickers microhardness (HV) for selected metals [Kanani, 2004]

Metal	Manufacturing process	
	Metallurgical	Electrodeposition
Cadmium	30	50
Chromium	350	1000
Cobalt	200	500
Copper	50	150
Nickel	150	500
Zinc	30	130
Tin	10	10

The properties of electrodeposited metals often differ from those of cast or wrought metals. The former may have finer grains, higher hardness, better mechanical properties (tensile strength, ductility and Young's modulus), better electrical and magnetically properties and better corrosion resistance [Cavallotti et al. 2005]. The Vickers microhardness value is one of the simplest ways of demonstrating such differences. From the data in Table 2.2, it will be clear that electrodeposited metal coatings are uniformly harder than their counterparts prepared by other metallurgical methods. Electrodeposited chromium is much harder than the metal obtained by thermal means. Bright nickel is much harder, less ductile and has a higher tensile

strength than cast nickel [Kanani, 2004]. The mechanical properties of bulk metals may be varied considerably by heat treatment or mechanical working. The properties of electrodeposited metals also may be varied, but this is primarily achieved by altering the conditions of deposition.

To obtain particular interest from industry, the electroplated alloys must possess considerably better properties for a given application than pure metal electrodeposits to compensate for the increased difficulty involved in the operation of the alloy plating process. However, generally speaking, the properties of electrodeposited alloys are still not well known. This has led to applications based on their obvious characteristics. For example, electroplated brass and gold alloys are utilized because of their color; cobalt nickel alloys are used for their brightness. Many potential uses of electrodeposited alloys still need to be exploited, but these applications must await the gathering of more data on the properties of the alloys.

### **2.4.3 Corrosion of Electrodeposited Alloys**

Corrosion, according to the ASM Material Engineering is the chemical or electrochemical reaction between a material, usually a metal, and its environment that produces a deterioration of the material and its properties. The major requirements for good corrosion protection are high corrosion resistance of the coating material, a pore-free structure, and good adhesion.

#### **2.4.3.1 Corrosion of Coating-Substrate Systems**

The corrosion behavior of a coated part (a coating substrate system) is determined by the corrosion resistance of the coating material in the respective medium. However, this holds only for absolutely dense coatings that completely separate the aqueous corrosive medium from the underlying substrate material. In

practice, coatings and thin films show pores, pin holes. And other defects after their deposition, or they may be damaged by scratches or other wear mechanisms. Both types of defects allow the corrosive medium to contact the substrate material or interlayers and underlayers.

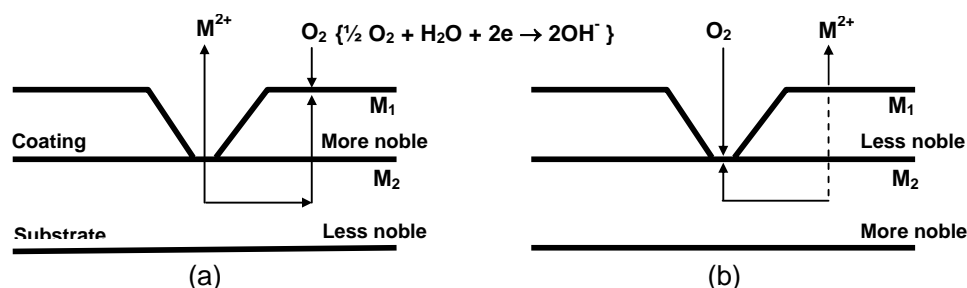


Figure 2.14: Schematic illustration of corrosion of coating substrate systems in the presence of pores. M, metal. (a) More noble coating on less noble substrate (galvanic corrosion). Increased corrosion of substrate material with small anodic area and large cathodic area. (b) Less noble coating on more noble substrate (anodic corrosion). Cathodic protection of substrate material, coating material dissolved, large anodic area, small cathodic area.

The relative corrosion behavior depends on the materials combination, the coating materials is either more noble or less noble than the substrate material, the corrosion medium, and the specific conditions [ASM handbook]. The electrochemical reactions are schematically illustrated in Figure 2.14. In the case of a more noble coating (Figure 2.14a), the corrosion medium reaches the substrate material, and a galvanic cell is formed between the anodic substrate material and the cathodic coating material. This results in strong local corrosion of the substrate.

### 2.4.3.2 Electrochemical Corrosion Test

Because corrosion of metals in an electrochemical process, electrochemical measurements are especially suited to it. The corrosion reaction occurs between the cathodic and anodic parts of a corroding system, resulting in an electric current in the metal and an ionic current in the electrolyte at the metal-electrolyte interface. The



amount of current produced is a measure of the oxidation or reduction reaction, so it provided information about the rate of the corrosion process.

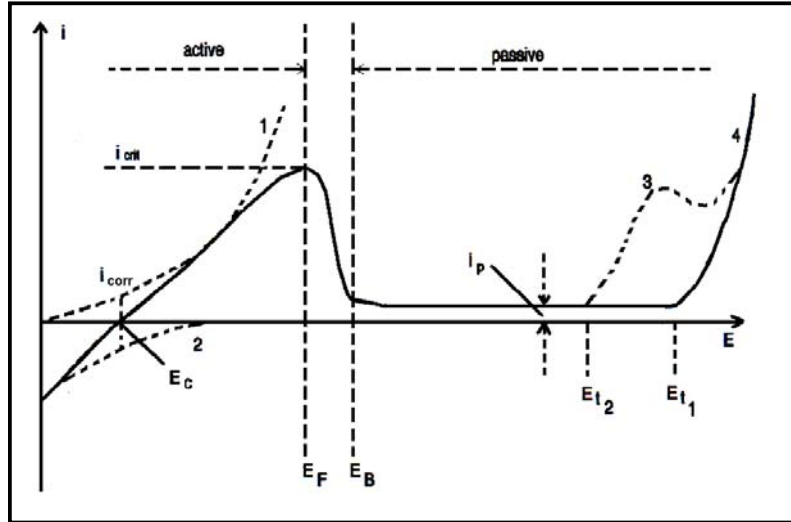


Figure 2.15: Current density vs potential curve for a typical metal electrode in neutral or acid solution. Active and passive regions are indicated with arrows [Wolf et al., 1995].  $E_{t1}$ : transpassive potential due to oxygen evolution on passive metal;  $E_{t2}$ : transpassive potential which indicates passive film dissolution.

Uniform corrosion of metals may occur as active or passive corrosion. The corrosion rate and the corrosion mechanism depend on many variables such as the electrochemistry of the metal surface, the composition and pH of the solution. A very important variable is the electrochemical potential at the surface of the corroding metal. Figure 2.15 shows the dependence of the current on the potential for a typical metal electrode in neutral or acid solution.

At  $E = E_{corr}$  metal continuously corrodes and the rate of this uniform corrosion is equal to  $i_{corr}$ . Curve (1) indicates the polarization behavior of anode process while curve (2) illustrates the polarization behavior of cathodic process. At  $E > E_c$  the dissolution rate rises strongly up to  $i_{crit}$ , the critical current (or critical current density) of the corroding surface. Around the corresponding potential  $E_F$  the metal surface is covered with a dense surface layer, mostly an oxide, which prevents a further increase

of the active dissolution. At more positive potentials the protective layer grows thicker and the decrease of the current indicates a very low corrosion rate in this passive state. The passive corrosion, with a very low passive current density  $i_P$ , extends over a rather broad potential region until the right hand side where there is oxidation of water (4) and for some metals transpassive dissolution (3) starts. The figure illustrates clearly the electrochemical processes at the metal surface to be strongly dependent on the potential [Wolf et al., 1995].

#### **2.4.3.3 Dealloying**

The selective dissolution of one component of an alloy (e.g. Zn from brass, Al from bronze, Cu from Cu-Au, etc) leads to substantial changes in the composition and properties of its surfaces. The corrosion process of various alloy systems has been studied by many researchers and reviewed and summarized by Pickering or a dual-element alloy system A-B, in the normal alloy content range (not extremely little A or B) [Ateya et al. 1996]. When selective dissolution occurs, the topmost layers of the alloy surface are depleted of the active component, and preferentially enriched in the more noble component of the alloy. Ateya et al. developed phenomena of selective dissolution, a some of the A atoms dissolve out of the topmost layer of the alloy, the remaining B atoms lose some of their A nearest neighbors. The extent of this loss depend on the prevailing potential, kinetic parameters of the dissolution of the A atoms as well as their mole fraction within the alloy. The remaining B atoms may be only mildly affected, become weakly bound to the lattice or, at the limit, become adatoms. The structure of the top most layer becomes defective, to varying degrees, because of the loss of the A atoms. As the concentration of the active component at the topmost atom layer decrease, a concentration gradient is established normal to the alloy-electrolyte interface. It drives the A atom from the nearest stoichiometric sub-surface layers to diffuse through the developing highly defective noble metal-rich layer towards the alloy surface and similarly the B atoms into the alloy, to support the reaction. The

repetition of this process, with deeper and deeper sub-surface layers, leads to the gradual and uniform thickening of the resulting noble metal-rich layer, to progressive depletion of the active metal in the surface region, and to continuous decrease of the dissolution rate of A with time.

## **2.5 Electrodeposition of Copper-Tin Alloys**

The available information concerning the electrodeposition of copper-tin alloy is virtually confined to the literature. Later claims concerning Cu-Sn alloy plating, however, have been based upon the use of both alkaline cyanide and acid sulfate electrolytes. Several recent reports on copper-tin cyanide and sulfate electroplating systems are reviewed in the following [Jacky, 1971; Helton et al. 1989; Pincincu et al. 2001]

### **2.5.1 Cyanide systems**

Jacky [1971] developed the electroplating of copper-tin-zinc alloy with cyanide system. The Jacky bath was comprised of 2.99-3.59 g/l  $\text{Cu}^+$ , 1.35-1.64 g/l  $\text{Zn}^+$ , 1.12-1.49  $\text{Sn}^{4+}$  g/l, 20.22-23.21 g/l NaCN and 29.95-74.89 g/l  $\text{Na}_2\text{CO}_3$ . This bath can be used for electrodeposition of a bright ternary alloy with composition generally in the range of 50-60 % wt. copper, 20-30 % wt. tin, 15-25 % wt. zinc, when plated at current densities of 5-45 ASF, temperature 120°-180° F and a pH of between 12.3-12.7 without the addition of the organic brightener [Jacky, 1971]. Product plated with the Jacky bath or its close equivalent was found to encounter severe tarnishing problems as they underwent a cleaning step prior to soldering.

Another patent gave a cyanide solution for plating an alloy of copper, tin, and zinc [Helton et al. 1989]. The preferred electroplating bath composition includes a predetermined amount of copper, tin, and zinc ions, and an effective amount of nickel

ions sufficient to promote the plating of corrosion resistant, bright silvery-colored plate of copper-tin-zinc alloy. Nickel is added to the bath to enhance the inclusion of tin within the plate alloy and is added at concentration between about 12.0 to 20.0 ppm (weight/volume). The practical implementation of the bath included 2.99-3.59 g/l  $\text{Cu}^+$ , 1.35-2.09 g/l  $\text{Zn}^+$ , 1.12-1.49  $\text{Sn}^{4+}$  g/l, 23.21-26.21 g/l NaCN and 4.49-5.61 g/l NaOH, plated at current density between 2-10 ASF and temperature 150° F (66° C). The bath aims at obtaining an alloy of 60-70 % wt. copper, 20-30 % wt. tin and 5-10 % wt. zinc, by Auger analysis using pure metal standard. The addition of sodium carbonate appears to be optional. Since sodium carbonate is a by-product of the plating process and appears in bath during plating. Test plates run as well run on bath composition having 30 ppm nickel to produce a tarnished brown plate in areas of high current density.

Copper-tin-zinc alloy codeposition using the chemistry of a commercial alkaline cyanide system was studied by Pincincu et al. [2001]. The voltammetry, the deposit composition and the morphology was investigated as a function of the concentrations of the three metal ions, Cu(I), Zn(II) and Sn(IV) as well as the concentration of cyanide, hydroxide, carbonate and Copper Glo additive. Over a range of temperature and current density (or potential), deposits that were adherent, silver in colour and highly reflecting could be produced and their composition in the range 47-51% wt. copper, 8-12 % wt. zinc and 38-43 % wt. tin. The desired silver colour required control of the alloy composition and an acceptable rate of deposition necessitated the use of a temperature above ambient (333 K). The Copper Glo additive has the role of improving reflectivity without changing the composition of the alloy.

### **2.5.2 Sulfate systems**

A non-cyanide sulfate copper-tin alloy plating bath has been developed, which has the advantage of low toxicity and relative ease of handling [Paunovic et al. 1998; Finazzi et

al. 2004; Survila et al. 2004). However, the electrolytes investigated have limitations, such as susceptibility to corrosion, low solubility of copper and tin, bath decomposition and the need for various additives, for example polyalcohol to improve the bath properties and result in high quality deposits. Copper-tin plating bath containing sorbitol as ligand has been developed by Finazzi [2004]. Bright reddish copper-tin electrodeposited were successfully obtained with the deposit have a maximum of ~ 3% of tin and that sorbitol was not incorporated in the deposit. The kinetic studies showed that copper (II) species control the electrochemical process of the copper-tin deposition and that this reduction process is controlled by mass transport, with a diffusion coefficient of  $8.1 \times 10^{-8} \text{ cm}^2 \text{ s}^{-1}$ .

Survila et al. [2004] developed co-deposition of copper and tin from Acidic Sulfate solution containing polyether Laprol 2402C. The electrolytic baths contained 0.01 M  $\text{CuSO}_4$ , 0.01 M  $\text{SnSO}_4$ , 0.6 M  $\text{H}_2\text{SO}_4$ , 50 mg/l of Laprol and various amounts of potassium halides ( $\text{Cl}^-$ ,  $\text{Br}^-$ ,  $\text{I}^-$ ) to help efficiently control the composition of bronze coatings. Introducing halide reduces the potential at which the copper and tin co-deposition begins and narrows the potential range for producing deposits of yellow bronze that contain 8-10% of tin. The optimum concentration of potassium halide for controlling the composition of bronze coating decreased in the series  $\text{I}^- < \text{Br}^- < \text{Cl}^-$ .

### **2.5.3 Plating Bath Selection**

It has been mentioned previously in Chapter I, in electrodeposition of alloys, the electrolyte and deposition conditions are chosen so that deposits have uniform composition and properties over the course of the deposition process. Based on equilibrium potential-pH diagrams for the systems  $\text{Cu-H}_2\text{O}$ ,  $\text{Sn-H}_2\text{O}$ ,  $\text{Zn-H}_2\text{O}$  and  $\text{Ni-H}_2\text{O}$  which are presented in Figure 2.16, 2.3, 2.17 and 2.2 respectively, electroplating can be done either in acid or in alkaline solutions. In acid solution electroplating may be conducted by reducing simple cations ( $\text{Cu}^{2+}$ ,  $\text{Sn}^{2+}$ ,  $\text{Zn}^{2+}$ ,  $\text{Ni}^{2+}$ ) while in alkaline

deposition must be conducted by reducing complex anions such as  $\text{HCuO}_2^-$ ,  $\text{CuO}_2^{2-}$ ,  $\text{HNiO}_2^-$ ,  $\text{SnO}_3^{2-}$ ,  $\text{HZnO}_2^-$  and  $\text{ZnO}_2^{2-}$ . Electroplating of metal/alloy from simple cation onto non planar metal substrates tends to produce a non-uniform coating because local deposition current density at location close to anode will be significantly higher than that at locations far from the anode. Basically ternary Cu-Sn-Ni alloy can be co-deposit during electroplating even though it should be done under mass transport control of copper ion. Zinc is not expected to be deposited simultaneously with the copper because its deposition potential is too low. It should be noted that no Cu-Sn-Ni-Zn alloy deposition will occur except the deposition potential of copper can be lower close to Sn, Zn, and Ni.

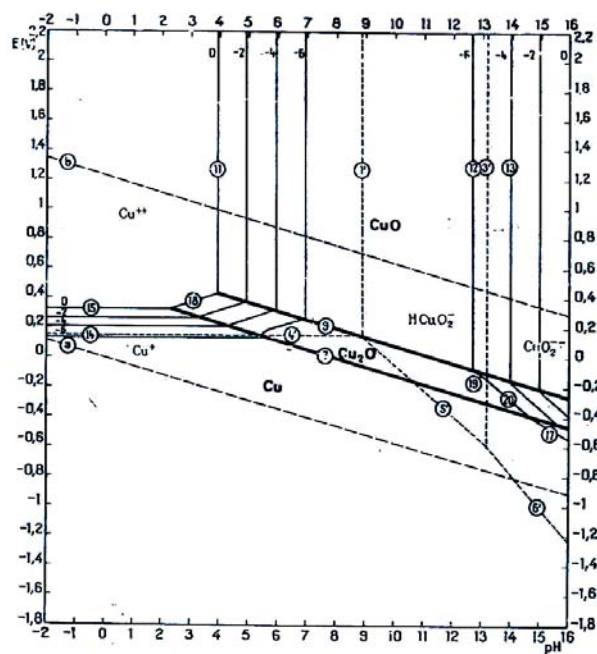
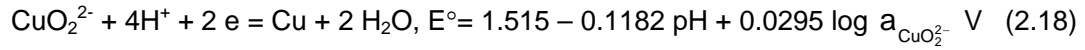
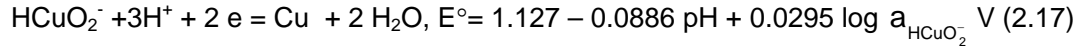


Figure 2.16: Potential–pH diagrams for Cu–H<sub>2</sub>O system at 25 °C [Pourbaix, 1974]

Deposition of copper from alkaline solution is disfavor due to the solubility limit of copper ions. At pH of about 13 (Figure 2.16), the copper ions appear as  $\text{HCuO}_2^-$  and  $\text{CuO}_2^{2-}$ . Their solubility limits at this pH are  $< 10^{-5}$  mol/L. Electrodeposition of copper from this solution might resulting copper powder adherence to substrate. As a

consequent, it is not convenient to electrodeposit copper from alkaline solution. Moreover, the equilibrium reduction potentials (E) of those anions at 25 °C are influenced by pH and their relationships may be expressed as follows;



These equilibrium reduction potentials are markedly higher than those for  $\text{HNiO}_2^-$ ,  $\text{SnO}_3^{2-}$ ,  $\text{HZnO}_2^-$  and  $\text{ZnO}_2^{2-}$  which can be examined in the equilibrium potential-pH diagrams Figure 2.2, 2.3 and 2.17, respectively. Therefore, co-deposition of copper with these ions, especially with zinc cannot be conducted from simple alkaline solutions. On the other hand, copper cyanide can be dissolved in the presence of excess cyanide to form cyanocuprate ions  $\text{Cu(CN)}_2^-$ ,  $\text{Cu(CN)}_3^{2-}$  and  $\text{Cu(CN)}_4^{3-}$  in alkaline solutions. Since the stability of these species is influenced by pH and potential, potential-pH diagrams presented in Appendix A are required to discuss their stability region and their equilibrium reduction potentials.

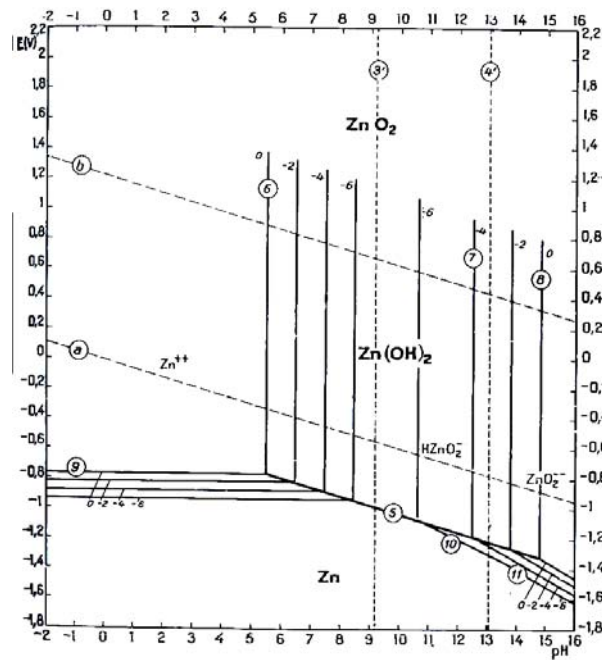


Figure 2.17: Potential-pH diagrams for Zn-H<sub>2</sub>O system at 25 °C [Pourbaix, 1974]

As shown in those potential pH diagrams, with increasing CN:Cu mole ratio, the distribution of copper cyanide species shifts more completely to the highly coordinated complex  $(\text{Cu}(\text{CN})_4^{3-})$  at a high cyanide concentration than that at low cyanide concentration. The equilibrium reduction potential of cyanocuprate ions decreases with increasing CN:Cu mole ratio. Increasing the pH is similar to increasing free cyanide concentration. In contrast, increasing temperature results in decreasing stability constants, therefore the distribution of copper cyanide shift to the lowly coordinate complexes. Because the reduction potential of cyanocuprate ions can be markedly lowered, e.g. by adjusting Cu:CN mole ratio in the electroplating bath, deposition of copper can be simultaneously occur with tin, nickel and even zinc and binary Cu-Sn and quaternary Cu-Sn-Zn-Ni alloys coatings can be developed in many metal substrates.

Tin can be deposited from  $\text{SnO}_3^{2-}$  which is dissolved in alkaline solution as shown in equilibrium potential-pH diagram Figure 2.3. Its solubility increases with increasing pH. However the solubility of this ion is limited because the more stable oxide ( $\text{SnO}_2$ ) might be precipitated. This tin ion is not influenced by the presence of cyanide ions. The equilibrium potential-pH diagram for the zinc-water system also exhibits the solubility of both  $\text{HZnO}_2^-$  and  $\text{ZnO}_2^{2-}$  ions is increased with increasing pH.  $\text{ZnO}_2^{2-}$  ions is predominant in very alkaline solution ( $\text{pH} > 13$ ).

More uniform deposit can be obtained for the electroplating which is influenced by mass transfer of cation toward the cathode especially at locations closer to anode. The rate of mass transfer of the cation may be formulated as follow:

$$J_T = J_C + J_D + J_M \text{ (mol/cm}^2 \text{ sec)} \quad (2.20)$$

where  $J_T$ ,  $J_C$ ,  $J_D$ , and  $J_M$  are total flux of ion, convection flux, diffusion flux and migration flux, respectively. In contrast electroplating from complex anion from alkaline solution will tends to produce more uniform coating because the complex anion will migration



away from the cathode and the rate of migration will be higher at locations closer to anode.

$$J_T = J_C + J_D - J_{M+} \text{ (mol/cm}^2 \text{ sec)} \quad (2.21)$$

This phenomenon is also appeared during electroplating using alkaline cyanide solution. It is also contributed by the presence of cyanide ions that can create the condition at which the deposition of copper from highly coordinated complex  $\text{Cu(CN)}_4^{3-}$  is disfavor. Electroplating from alkaline solution including alkaline cyanide bath will have advantages such as (1) electroplating bath has higher covering power; (2) more uniform thickness coating can be formed on non planar substrate; (3) solution is not very corrosive compared to acid solution; (4) Mostly hydrogen evolution is more difficult to from. Therefore the coating is less brittle than that produced in acid solution.

Alkaline cyanide baths have been selected in this research works. Beside those advantages the utilization of cyanide baths allow the electroplating of quaternary Cu-Sn-Zn-Ni alloys can be conducted.

#### **2.5.4 Properties of Copper-Tin Alloys**

Copper-tin alloys are materials that have good corrosion resistance, malleability, ductility and solderability. These alloys are used industrially for metal coating, with the aim of conferring corrosion protection and mechanical properties to the substrate and therefore the proportions of copper and tin in the alloy are of fundamental importance in obtaining the desired characteristic [Finazzi et al., 2004].

White Miralloy coatings contain about 55 % of copper and 45 % of tin, or 55 % of copper, 30 % of tin and 15 % of zinc. Yellow Miralloy coatings as alloy components on an average contain 80 % of copper, 17.5 % tin and 2.5 % of zinc, or 85 % of copper, 10 % of tin and 5 % of zinc, or 85 % of copper and 15 % tin. Miralloy coatings are characterized by an excellent thickness distribution even in the case of parts with

complex shapes. The coating hardness of Yellow Miralloy and White Miralloy are 400 HV 0.1 and 550 HV 0.1, respectively [<http://www.umicore-galvano.com>].

The coating is extremely abrasion-resistant, for this reason Yellow Miralloy coatings are particularly for coating bearing shells or piston. White Miralloy coatings exhibit an acceptable contact resistance, for this reason they are used for coating connectors in the motor industry. The solderability of the coating is good with suitable fluxes. Furthermore, the coatings are diamagnetic. Therefore connectors for high-frequency technology provided with Miralloy coatings reach very low intermodulation values in the mobile radio frequency range. Copper has become the metal of choice to meet the needs of present and future generation devices. In order to further improve the intrinsic resistance of copper to EM/SM induced failure, researchers have attempted to introduce various alloying elements into copper lines.

Copper has become the metal of choice to meet the needs of present and future generation devices. The copper-tin system has shown significantly higher electromigration lifetimes and activation energy than pure copper. The continuing shrink in device size, the copper-tin has generated great interest to create interconnects with low resistivity and superior electromigration (EM) and stress migration (SM) lifetimes in comparison to the existing Al or Al-alloy interconnections [Padhi et.al. 2003]. Hu et al. [1995] studied the impact of addition of Mg, Sn, and Zr on the EM of sputtered copper lines. They concluded that the drift velocity of copper increased by addition of Mg, while addition of Sn and Zr resulted in reduction of drift velocity. Activation energy for EM of copper increased from 0.75 to -1.3 eV with addition of 1 wt. % Sn, while the resistivity increased to 4.1 mV/cm<sup>2</sup>. Furthermore, due to the low solid solubility of tin into copper, the copper-tin system is amenable to heat treatment to produce precipitation of intermetallic phases and segregation of solute species to grain boundaries, thereby, reducing the aggregate resistivity of the alloy. In

addition to improved resistance to EM induced voiding, copper-tin alloy films have superior resistance to corrosion, which is very desirable in the processing of multilevel Cu-wiring.

## **2.6 Electrodeposition of Multilayers**

Multilayer alloys are the materials which consist of multiple alternate layers of at least two suitable metals/alloys. These materials have been found to possess outstanding properties, such as enhanced tensile strength and microhardness, and improved wear resistance [Tench et al. 1984, 1991; Ebrahimi et al. 1998; 2001]. The enhancement is attributed to the unique multilayered structure of these composites, i.e., the blocking effect of the structure to dislocation glide from one layer to another. The merit of this structure is that the composition and properties of its component layers can be adapted individually. Thus, the properties of the composites are designable and predictable. By choosing suitable combination of the metals and appropriate processing parameters, the nature of the interface between the layers can be modified also. Two possible processes can be considered in electrodeposition of metallic multilayers, single bath and dual bath technique.

The single-bath technique, in these processes only multilayers with elements capable of being electrodeposited from a one electrolyte containing both elements can be produced [Haseeb et al. 1992; Roy, 1998; Miyake et al. 2001]. A pure metal and an alloy of first metal and a second less noble metal are plated successively by changing the current density, by controlling diffusion near the cathode surface, by changing the agitation or by a combination of these parameters [Haseeb et al. 1992; NabiRahni et al. 1996]. The deposition potential of the two constituents should be far enough apart allow the separated deposition of each element. The single bath technique is in fact a pulsed plating process in which at higher overpotential or current the less noble

constituent, and at lower overpotential or current the more noble constituent are deposited [Haseeb et al. 1992].

Lashmore and Dariel [1988] prepared Ni/Cu multilayered coatings from single nickel sulfamate electrolyte with added copper content. Their processing was based on the disparity in standard potentials of nickel and copper, which is given in Table 2.1. According to this table,  $E^\circ \text{Cu}^{++}/\text{Cu} = +0.34 \text{ V}$ , and  $E^\circ \text{Ni}^{++}/\text{Ni} = -0.25 \text{ V}$ . There is a potential gap between Cu and Ni, and Cu is a more noble element than Ni. If the cathode potential is between  $+0.34 \text{ V}$  and  $-0.25 \text{ V}$ , only copper ions can discharge. If the cathode potential is more negative than  $-0.25 \text{ V}$ , both copper and nickel can be deposited. However, if the copper ion concentration is much lower than that of nickel, and the deposition time is very short, only nickel can be deposited in the latter case. This is because the copper deposition is controlled by copper ion diffusion from bulk solution to the vicinity of the cathode surface. Therefore, by controlling the cathode potential, copper ion concentration, and the deposition time, nickel and copper can be separately and alternately plated on the same substrate from a single electrolyte. Their nickel sulfamate electrolyte contained 90 g/l Ni, 0.9 g/L Cu in the form of copper sulfate, and 30 g/L boric acid at pH ranging from 3 to 3.5.

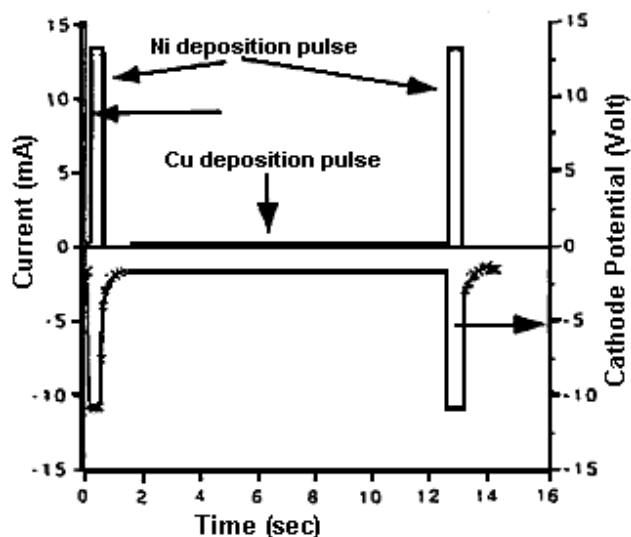


Figure 2.18: The current pulse electroplating of Cu/Ni multilayered composites.

A platinum sheet was used as the anode, and a copper single crystal sheet was employed as the cathode substrate. The cycle consisted of a short and high current pulse for depositing the nickel layer, and a long but low current pulse for depositing the copper layer (Figure 2.18). Between them, a short, zero current pulse was designed to improve the sharpness of the nickel-copper interface. Copper was deposited at  $0.3 \text{ mA/cm}^2$  and nickel at  $12\text{-}20 \text{ mA/cm}^2$  current densities. The thickness of each Cu or Ni layer was about 10 nm. An overall thickness of  $15\text{-}20 \text{ }\mu\text{m}$  was deposited [Lashmore et al. 1988].

The dual-bath technique employs two separate electrolytic plating baths. The substrate is successively transferred between separate plating baths and each layer is deposited alternately to laminate the sublayer from the relevant bath. The plated parts are activated prior to entering the first solution, plated and subsequently rinsed and activated all again before entering the second solution [Haseeb et al. 1994; Wang 1997]. Interesting results using dual bath technique have recently been published by Haseeb et al. (1994). They conducted electrodeposition of Cu/Ni compositionally modulated Multilayer with sublayer thickness in the nanometer range. Electrodeposition of copper was carried out in a copper sulfate bath ( $90 \text{ g/l CuSO}_4 \cdot 5\text{H}_2\text{O}$  and  $200 \text{ g/l H}_2\text{SO}_4$ ) while nickel was deposited from a nickel sulfamate bath ( $400 \text{ g/l Ni(NH}_2\text{SO}_3)_2$  and  $30 \text{ g/l H}_3\text{BO}_3$ ) both maintained at temperature  $30 \text{ }^\circ\text{C}$ . Both copper and nickel were deposited galvanostatically at a current density of  $20 \text{ mA/cm}^2$  and the thickness of copper and nickel sublayers were kept equal.

In the single bath technique, the type of ion discharging on the cathode surface is determined by the electrochemical potential and mass transport (ion diffusion). The major merit of this process is high efficiency, especially for the deposition of nano-scale multilayers. However, not any two metal combinations can be deposited in this way because of the requirement of a relatively wide standard

electrode potential gap between the two metals. Since co-deposition is not completely eliminated, the concentration profile at the interface can not be very sharp. Although it is very efficient in thin layer deposition, this method may not be applicable to thick layered specimen preparation because the pulse time of the less noble species is limited by the diffusion of the more noble species. Other difficulties involve the designing of the electrolyte composition and the maintenance of the concentration ratio of the two metal ions. These difficulties and limitations prompt us to use another process in which two metals are deposited alternately from two separate electrolytes.

### **2.6.1 Compositionally Modulated Multilayer Alloy Applications**

Compositionally modulated multilayer alloy are the materials which consist of multiple alternate layers of at least two suitable metals. These composites have been found to possess outstanding properties, such as enhanced tensile strength and microhardness, and improved wear resistance [Tench et al., 1991]. The enhancement is attributed to the unique multilayered structure of these composites, i.e., the blocking effect of the structure to dislocation glide from one layer to another. The merit of this structure is that the composition and properties of its component layers can be adapted individually. Thus, the properties of the materials are designable and predictable. By choosing suitable combination of the metals and appropriate processing parameters, the nature of the interface between the layers can be modified also. Therefore, mechanical properties of these multilayers can be controlled over a wide range.

Several measurements of mechanical properties of metallic multilayers have been conducted. These works involved indentation microhardness measurement and tensile tests [Tench et al., 1991]. A common conclusion made from these tests was that, as the layer spacing decreases, the tensile strength and microhardness of the materials increase. The enhancement effect was attributed to the influence of the

interfaces of micro-layered structure to dislocation behavior. Two general models were employed to explain this effect. One is Koehler's modulus theory which indicates that the interfaces of multilayered structure can offer strong barrier to dislocation glide from lower modulus metal to higher modulus metal when two moduli differ greatly. He found a relation for the minimum shear modulus required for dislocation transmission to occur as,

$$\mu_{\min} \approx \frac{\mu_b}{8\pi} \frac{\mu_a \mu_b}{\mu_a + \mu_b} \quad (2.22)$$

where  $\mu_a$  is the shear modulus of material a,  $\mu_b$  is the shear modulus of material b. Another is the Hall-Petch relation which gives the dependence of the strength on the layer spacing where the image force increases with decreasing layer spacing. Hall-Petch relation is expressed as,

$$\sigma_Y = \sigma_0 + Kd^{-n} \quad (2.23)$$

where  $\sigma_Y$  is the yield strength of materials,  $d$  is the thickness of layers,  $\sigma_0$  and  $K$  are the constants related to the properties of the materials,  $n$  is the exponential which is typically taken as 0.5. Hall-Petch relation is applicable to most bulk polycrystalline materials during low-temperature deformation. For multilayer, this relation also gives reasonably accurate prediction of the dependence of strength on layer spacing. However, as the layer spacing is reduced below a critical value, the tensile strength of the composites even decreases with decreasing the layer thickness. This loss in strength enhancement was attributed to incoherence or misfit dislocation formation at the layer interfaces.

Tench et al. [1991] studied the tensile strength of Ni/Cu multilayered alloys. A wide range of copper layer thickness, from 3.20 to 0.01  $\mu\text{m}$ , was prepared but the composition was always controlled at 90%Ni-10%Cu. The total thickness of deposits was about 50  $\mu\text{m}$ . The tensile test data, shown in Figure 2.19 [Tench et al. 1991], indicated that the tensile strength remained practically constant at about 600 MPa

down to a thickness of about 0.4  $\mu\text{m}$ , and then increased sharply to about 1300 MPa for thicknesses in the 0.01  $\mu\text{m}$  range. Pure nickel specimens deposited from the same bath were also tested. The measured tensile strength was always  $< 400$  MPa, indicating that the multilayered structure yielded a factor of three time improvement.

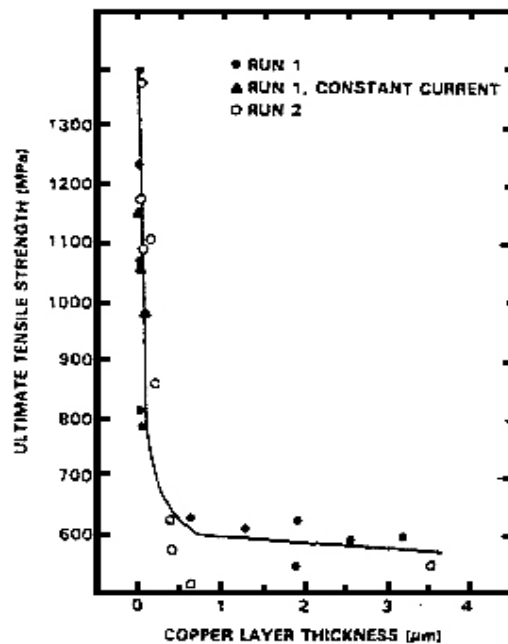


Figure 2.19: Tensile strength vs. copper layer thickness for 90%Ni-10%Cu electrodeposited multilayered [Tench et al. 1991]

Drastic changes in tensile strength, ductility and other mechanical properties have been reported by a number of researchers. Other, perhaps even more interesting properties such as magnetic, optical, physical and chemical properties are known to change as well. Compositionally modulated alloy and/or laminated nanostructures can be looked upon as new materials because the two alternating metals in the structure are constantly blocking the formation of the individual structure that each of the two metals would approach if allowed to form in the pure state [NabiRahni et al. 1996]. Some of the most promising compositionally modulated alloy results indicate several interesting applications:



- (i) The use of structures with high tensile strength or corrosion resistance in micromechanics, with such potential applications as biocompatible, implantable drug delivery pumps in medicine;
- (ii) Information storage devices using a perpendicular, i.e. out-of-plane orientation of the magnetization vector to create true vertical recording (for hard discs) also, for nanomizing chip circuit designs and magnetic thin films;
- (iii) Optical devices such as laser mirrors or mirrors for long-wavelength neutrons;
- (iv) Implantable micromechanical pumps for monitoring and drug delivery.